POLITECNICO DI TORINO

Master's Degree in Mechatronic Engineering

Master's Degree Thesis

Mechanical and Control Design of a Flexible Modular Gripper

Supervisors

Prof. Marina INDRI

Supervisors at Comau

Ing. Vito BORRELLI

Ing. Francesco BECCARISI

Candidate

Antonio TROIANO

December 2023

Abstract

The current thesis is carried out in collaboration with Comau S.p.A, the main focus of the work is to propose a model of a vacuum gripping device, characterized by modularity and flexibility. The gripper has to be used in the depalletizing process of several lines, each line is characterized by a different pallet layout, different sizes of the boxes, and different masses. The first phase of literature research provides a generic view of pneumatic gripping devices, their classification, and shows some of the proposed solutions regarding similar problems, where the design of a vacuum end effector is needed. After the review of the proposed solution, it is chosen to develop a flexible gripper, able to to adapt itself to the different boxes of the lines, and composed mainly of elements available on the market. Regarding the actuation, an electric stepper motor is preferred, with respect to a hydraulic or pneumatic actuator, given its simple positioning that can be managed by the motor controller itself. The first phase of the design consists of the definition of a pneumatic system to provide the required vacuum in the suction cups, a system composed of three vacuum zones is produced, to adapt to the sizes of the boxes and prevent the total vacuum loss in the case of leakage occurring, the gripper uses ten suction cups, divided into two three-cups sections and one four-cups section, each vacuum zone has a corresponding vacuum generator, selected considering the required pressure to guarantee the grasp of the box even when not all the suction cups have a proper sealing. The mechanical design consists of the 3D modeling of some components such as the main plate, or different mountings and adapters, which the bought components can be mounted on. A digital mock-up of the gripper is produced using SolidWorks, the suction cups of the gripper are distributed on two extruded profiles, in this way it is possible to simply change the number or type of cups, or the dimensions of the gripper substituting the extruded profiles which are moved symmetrically by an electric axis, to adapt to the box sizes. The last part of the work consists of the definition of the necessary electronic components: the stepper motor, the motor controller, the pressure sensors, and the optic sensors to detect the boxes. It is then defined how the elements are connected and how the gripper is interfaced with the robot. For the control of the gripper it is chosen to exploit the additional digital input and output ports of the robot controller, all the electronic devices on the gripper, including the vacuum generators, can send or receive a digital signal to be activated or communicate their readings. A set of PDL2 routines is developed using the software Roboshop by Comau, the routines can be called by the robot program to obtain information about the sensor, toggle the vacuum generation, and move the suction cups. The proposed concept represents a vacuum-based gripping device, flexible and modular, the production of

a prototype could verify the performances of the solution in a real-world scenario; future development could focus on the implementation of a fieldbus communication with the robot.

II

Acknowledgements

I would like to express my gratitude to those who have contributed to my thesis work. I thank my supervisor, Professor Marina Indri, for providing me with the opportunity to embark on this journey and for the guidance she has given me. I extend my thanks to my supervisors at COMAU, Ing. Francesco Beccarisi and Ing. Vito Borrelli, for welcoming me into their work environment and for guiding me throughout this experience. I also express my gratitude to the company COMAU for this opportunity, and to all the workers that I met, whose knowledge and experience were valuable for my work.

Finally, I thank all my loved ones: first and foremost, my mother, for her sacrifices that have allowed me to come this far and for her constant support. Then, my aunts and uncles, and cousins, who have always encouraged me despite the distance and challenges. I also thank my friends, both old and new, near and far, for being my home, advisers, and family.

Table of Contents

List of Tables

List of Figures

Chapter 1

Introduction

Robotic grippers are tools attached to a robot's wrist. They are used to interact with the environment, in particular for operations that involve manipulation and movement of objects. Robotic grippers can hold objects using different principles, among the most common typologies, there are jaw grippers, vacuum grippers, magnetic grippers, and anthropomorphic grippers. The selection of the gripper depends on the task to be performed. The thesis realized in collaboration with COMAU SPA, focuses on the design of a robotic gripper to be used in a depalletizing solution. The designed end effector uses suction cups to grasp cardboard boxes of different dimensions and weights, it is composed of custom-designed parts and commercially available components. The device is characterized by the possibility of changing the position of the suction cups and the presence of different vacuum zones, that allow the gripper to be suitable for different grasping scenarios. The configuration of the gripper, in terms of the number of suction cups and working dimensions, can be changed, thanks to the utilization of standard components available on the market. Some proposed models of vacuum gripping devices are analyzed in Chapter 2, where it is also reported a general classification of pneumatic gripping devices. Chapter 3 describes the analyzed problem. The objects to be moved by the gripper and their layouts in the different pallets are shown; then the fundamental aspects of the gripper are presented. Chapter 4 reports the procedure followed to define the vacuum system and shows the components present in the vacuum circuit. Chapter 5 focuses on the mechanical design of the gripper. The custom-designed parts are described and it is shown what commercially available products are needed. In this chapter are also reported the procedures regarding the verifications performed on the components. In the end, it is shown a mock-up of the gripper. Chapter 6 focuses on the electronic architecture of the gripper: the working principle of the utilized devices is described and it is shown how they are integrated with the robot. In this chapter, it is also described the realized PDL2 library, which is used to control the gripper by the robot cabinet.

Chapter 2

State of the art

This chapter analyzes the state of the art regarding gripping devices. The first part focuses on the classification of pneumatic gripping devices, showing the main characteristics of such devices and their differentiating factors. The second part focuses on some of the proposed solutions regarding vacuum grippers available in literature and describes their characteristics.

2.1 Pneumatic gripping devices in the industrial robots field

The analysis in [1] represented a starting point for the thesis work giving a general view on the currently available technologies in the field. The authors provided a classification of Pneumatic Gripping Devices used for industrial robots. The classification is based on different features, such as the type of pneumatic gripping device, the type of contact with the working object, the method to center the object, and others. The first distinction is focused on the type, or better, the technology that generates the lifting force on the working piece. The authors identify three families of pneumatic gripping devices:

- Vacuum Gripping Devices: they provide the lifting force exerting a vacuum on a section of the object surface using a sucker elements such as a suction cup or a pad and so on.

- Jet Gripping Devices: the lifting force is produced using a stream of pressurized air applied to the object.

- Combined Pneumatic Gripping Devices: they use different kinds of technologies together.
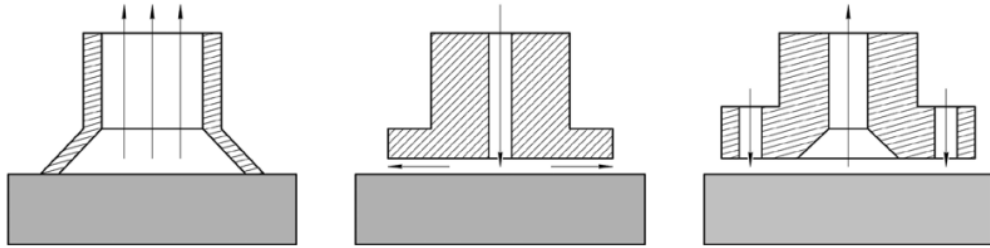
Figure 2.1: Classification according to the type [1]

The different types are sketched in Fig. 2.1 from [1], as listed.
Also the contact generated with the object represents a distinguishing factor.

- Contact device: where the gripping device and the working object have a mechanical iteration, exchanging forces across some surface.

- Low-contact device: where the portion of the gripping device generating the lifting force is not in contact with the piece, but some other element of the gripper prevents the displacement of the latter.

- Contactless device: where there is no mechanical contact between the gripper and the object and pneumatic principles are used to prevent displacement.

The different types can be seen in Fig. 2.2 from [1], as listed.
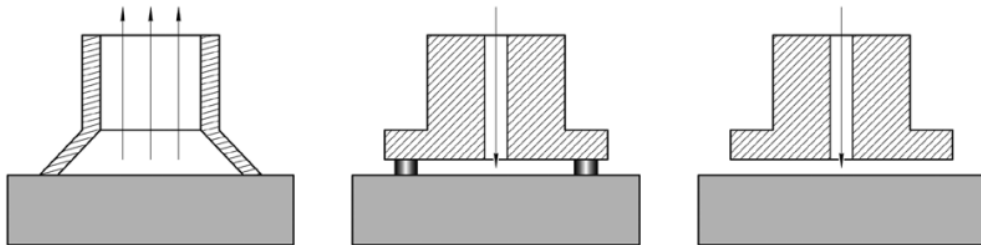
Figure 2.2: Classification according to the contact [1]

According to the positioning of the object on the device, the distinction is made between:

- Basing: the positioning is based on the definition of a surface of the object on which the force is applied.

- Centering: the positioning consists in the definition of an axis of symmetry of the object.
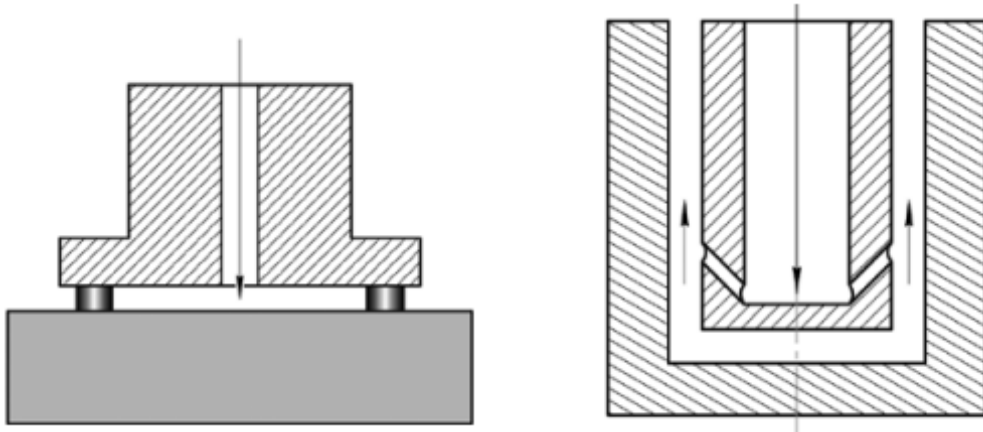
Figure 2.3: Classification according to the positioning [1]

The different types can be seed in Fig. 2.3 from [1], as listed.

Mykhailyshyn et al. in [1] also distinguish pneumatic gripping devices according to their specialization, classifying them in:

- Multi-purpose

- Targeted

- Special

It is trivial that the first ones provide lifting for objects of various sizes and shapes, the second are made for a narrower set of objects sharing the same structure, and the latter are suitable for only one working piece. Another distinction can be made, according to [1], depending on the operation range; in particular, wide-range grippers can deal with a big range of variability of the gripping surface, narrow-range have a more limited range. The number of working positions is also a differentiating factor, having single-positioning, as shown in Fig. 2.4, and multi-positioning technologies, depicted in Fig. 2.5.

Furthermore, the Multi Position Devices can be classified in sequential, parallel or combined action according to the timing or logic of operations done by the parts. Moreover, the control method provides another possible distinction:

- Command: the device can only grip or release the object.

- Programmable: the program can define relative position of the elements or the load capacity.

- Adaptive: using different sensors the gripper can adjust its parameters by itself.
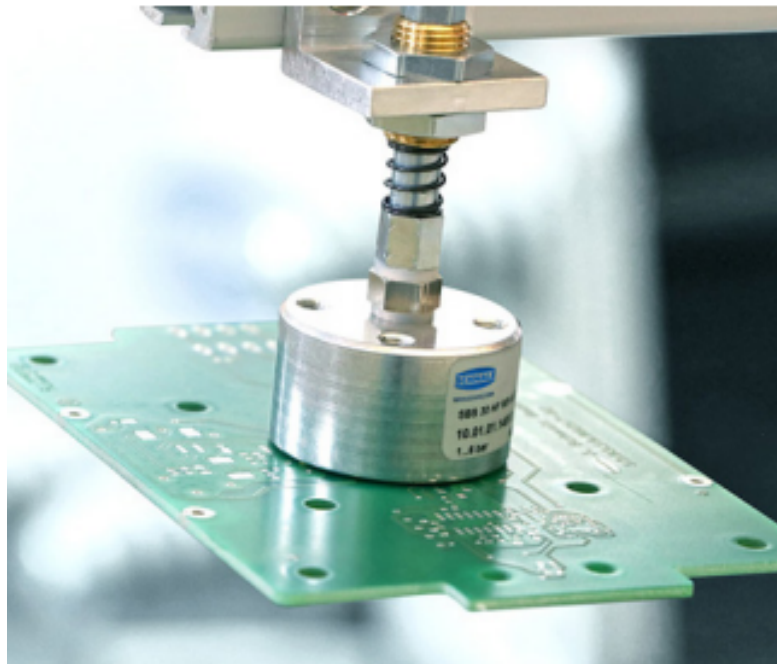
Figure 2.4: Single Position Gripping Device [1]
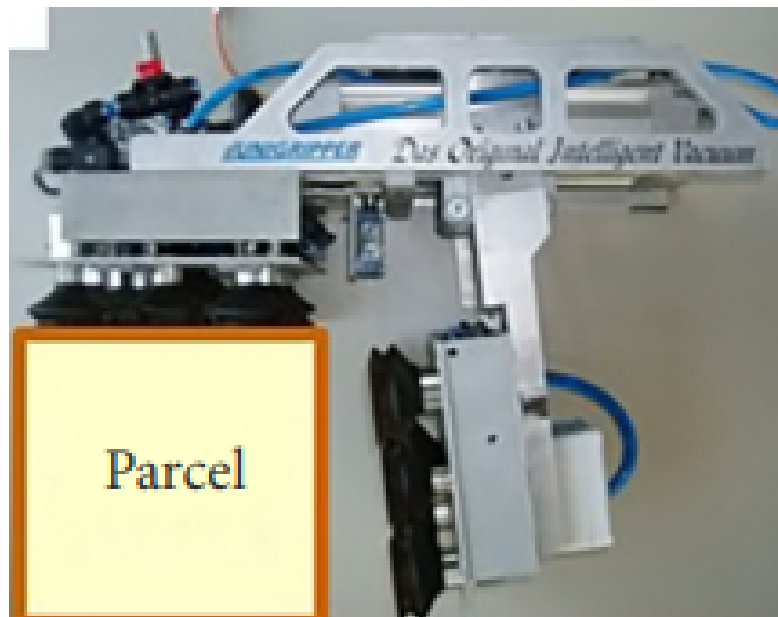
Figure 2.5: Multi Position Gripping Device [1]

2.1.1   Vacuum gripping devices

Vacuum Gripping Devices exploit the generation of vacuum directly on the object surface, under the suction cup, to produce a lifting force. The main advantages of this technology are its simplicity, the speed in the loading and unloading operations and a more distributed force on the piece compared to the mechanical grippers. The main utilization scenarios involve flat working objects, the grippers are usually equipped with various suction cups when dealing with bigger objects. Vacuum grippers can be again divided according to their suction cups material, type, or the technology used to create vacuum, referring to the latter element there are different possibilities available:

- Pump-less devices: in this case the vacuum is created modifing the geometry, of the gripping element, this means that the suction cup is not linked to any vacuum generator, but it sticks to the working element pressing on it and making the air under the chamber escape the volume; at this point the elastic material of the cup is able to generate a suction force.

- Piston devices: this technology requires the presence of a variable chamber attached to the suction cup, the movement of the piston inside the air-tight chamber generates a vacuum in the cup.

- Vacuum generator: these devices can use different principles to generate vacuum in the suction cup, such as Venturi, Coanda or use a pump or a fan.

The different technologies can be seen in Fig. 2.6. Mykhailyshyn et al. provide the graph reported in Fig. 2.7, which compares the performances of different typologies of vacuum generators, showing the obtainable vacuum levels and the evacuated airflow. It is clear that different technologies have different fields of application, advantages and drawbacks. Pumpless devices' performances are strictly dependent on the surface of the manipulated object, a smooth and regular surface is mandatory, similarly, the piston devices can only account for a limited amount of leakage between the suction cup and the object. For fan and vacuum pumps electrical components, such as electric motor and controllers, are needed to generate vacuum along with the need for bigger hoses, the main drawback of these systems is that a leakage in any point of the vacuum circuit leads to the depressurization of the whole circuit. With Coanda and Venturi ejectors, the vacuum generation can be decentralized, each suction cup can have its own ejector, solving the problem of total depressurization.
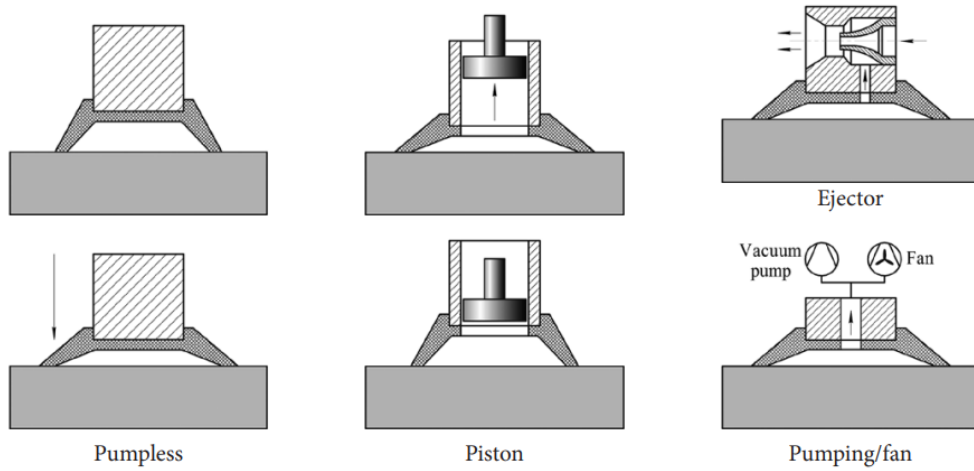
Figure 2.6: Different technologies for generating vacuum under the suction cups [1]
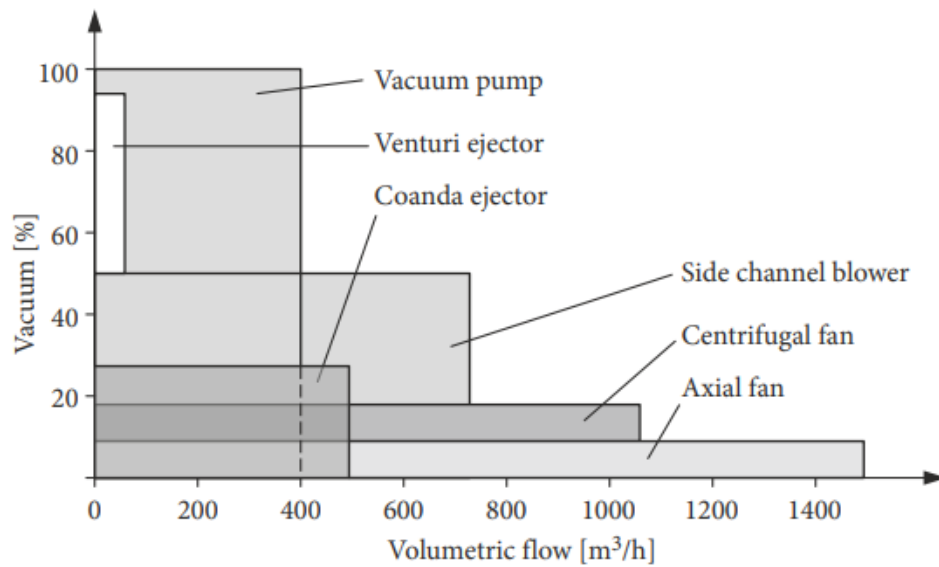
Figure 2.7: Different technologies capability of sucking air [1]

2.2 A comparison between a Vacuum and a mechanical gripper

Littlefield et al. [2] propose a comparison between two technologies of end effectors to be used in a warehouse picking process. The grippers are based on very different working principles: one is an under-actuated three fingers hand called *"ReFlex"*,

the other, called *"UniGripper"*, uses vacuum and has a degree of freedom being capable to move the suction element in a wrist like manner as shown in Fig. 2.8

Figure 2.8: ReFlex gripper and UniGripper [2]

The authors use a standard method to obtain grasping, using collision-free trajectories. In the experiments, a total of twelve different objects are used to test the reliability of the grasping, since each kind of gripper requires different trajectories and approach strategies. In the end, it is shown that the planning process influences the outcome of the grasp, the vacuum gripper proves to be suited for objects with a flat surface, whereas the robotic hand is more suitable for non-uniform objects.

2.3 Suction pad unit using a bellows pneumatic actuators

The work form Tanaka et al. [3] focuses on the realization of a gripper for a depalletizing robot. The main goal of the research is to develop a solution capable of working with multiple boxes at the same time and adapting to different heights of them. It is also important that the boxes are not crushed by the end effector due to the height differences, as well as the gripper should accommodate for various inclination of the working objects. The robot used by the authors is a linear-motion type, composed of a main arm, where the gripper is placed, that reaches the boxes, and a conveyor arm composed of multiple rollers where the box is placed and then moved to the follower conveyor. An image of this kind of solution is reported in Fig. 2.9. After the definition of the working conditions such as the maximum height difference between boxes, the masses and the maximum inclination,

Figure 2.9: Linear motion depalletizing robot [3]

the proposed solution is composed by a matrix of fifty suction cups (Fig. 2.11). Particular attention is directed toward the suction cup unit: to accommodate for the dimension differences of the boxes they must provide some vertical displacement, moreover, the suction cup itself has to be moved up or down and this is done using some bellow pneumatic actuator. Fig. 2.10 shows all the main characteristics of the component: the bellow actuator is expanded by the mass of the grasped object, and is retracted when a negative pressure is generated in its volume. Since the actuator is not capable of providing sufficient load resistance, a high-strength wire is connected between the unit base and the suction pad. Being shorter than the maximum length of the bellow actuator, the wire provides all the resistance to the load. When the actuator is retracted, if the load is too high, it can crush in the radial direction, so metal rings are placed in the actuator crests. The bellow actuator and the suction cup are driven separately, the unit is then tested for the requirements in terms of height difference, load capability, and inclination resistance.

Through various tests the authors show that the developed solution has multiple advantages when compared with common solutions: in case of height difference the pressing force on taller boxes is lower, the gripper has a higher capability of retraction thanks to the bellow actuators, and can be used with tilted objects.
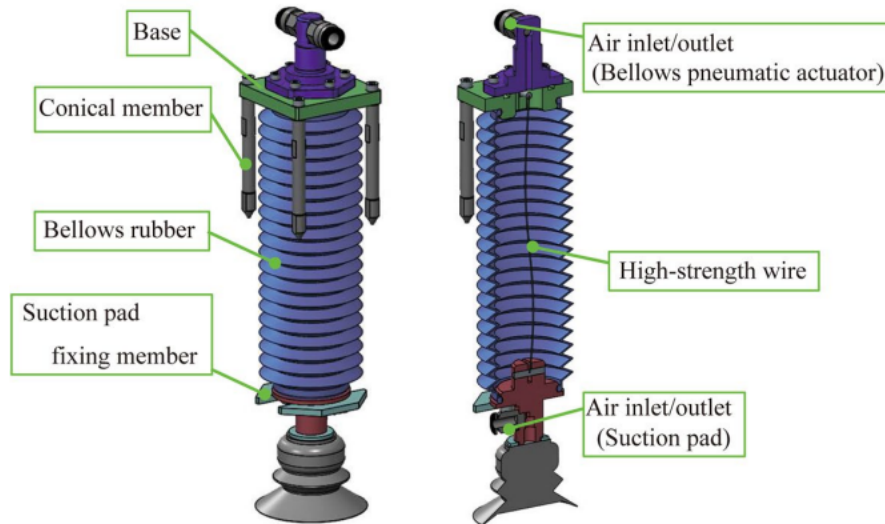
Figure 2.10: Proposed suction pad unit [3]
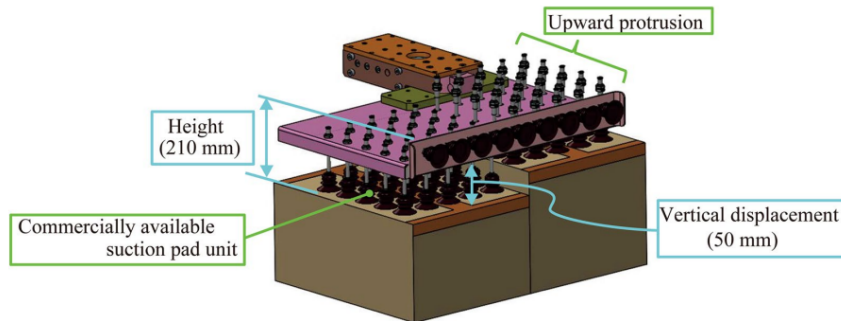
Figure 2.11: Proposed end effector [3]

2.4 Design of enlarging vacuum gripper using slider crank mechanism

Another model of vacuum grippers is proposed by Dhadge and Tilekar [4]. The gripper has two suction cups that contact the working object from the sides. The

piece is not sustained by the friction forces only, as usual for two fingers grippers, but the vacuum keeps the object in position. The author concludes that the possibility to change the suction cups position leads to a wider range of object that can be grasped; to implement this feature he proposes a slider and crank mechanism moved by an electric actuator. The suction cup units move along an angle arm thanks to roller bearings. The solution is shown in Figure 2.12.
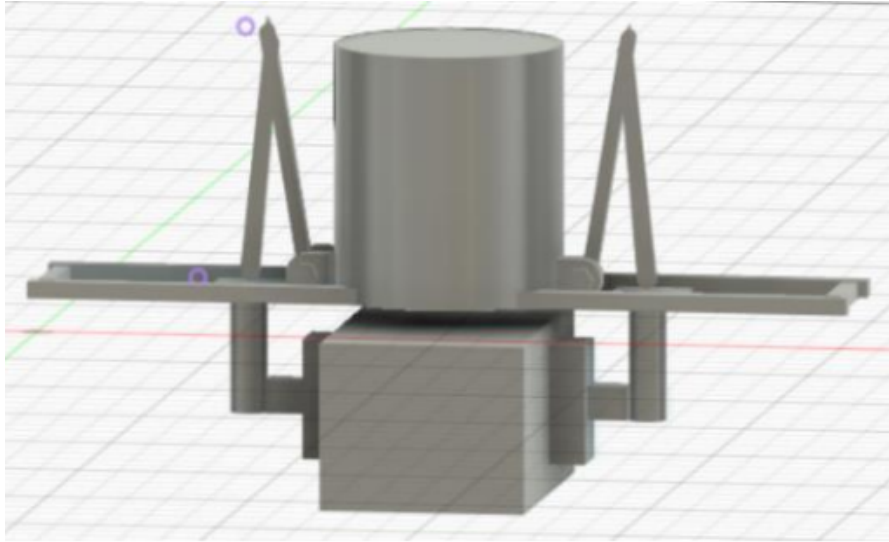
Figure 2.12: Proposed end effector [4]

2.5 Development of a modular, reconfigurable end effector for the plastics industry: a case study

In [5], the authors Saliba et al. address the problem of removing freshly produced plastic components from their molds. The aim is to produce a better solution to extract the components, perform a simple processing on them, and finally place them on a conveyor system. The current adopted solution consists of a cartesian robot equipped with a vacuum gripper and a jaw gripper, the first is used to extract the part from its mold, and the second is used to cut the runners from the part and dispose of them. The industry works in batches, using molds that produce from two to sixteen parts each. Given the variability of the produced plastic components, a different end effector is designed for each batch, the authors assert that the company uses a total of four hundred custom-built end effectors, with bad consequences on the needed storage and set up costs. In addition, when

a previously realized part has to be produced again, the corresponding end effector and control program have to be resourced. The new solution has to guarantee some specifications: perform the transferring operation, be able to work with hot components, not damage the parts, provide high accuracy, and be adaptable to other parts to be extracted in the future. The authors propose different solutions based on different principles. One of them is a Pin-box end effector. It consists of a matrix of pins that can retract when pushed against the plastic part. The pins that remain extended are then pushed toward the edge of the plastic part inflating a surrounding bladder. Another one is composed of a matrix of suction cups that works with a blanking plate to cut off the not needed cups. The last solution consists of a polymer pad filled with holes to be connected to a vacuum pump. With these solutions, the runners' removal is done by another tool. The authors also evaluate the utilization of a plug board where suction cups and jaw grippers can be added as needed and the utilization of reconfigurable rails where the components can be added as wanted. The latter solution is chosen to be developed, producing the CAD model reported in Fig. 2.13, it consists of two mounting rails on which cross rails are mounted. The suction cups are attached to the latter using sliding mounts to provide reconfigurability, the position is then locked using a spring-loaded pin. A similar solution is also used to position the mounting rails on the cross rails. The paper highlighted the differences between fixed, reconfigurable,

Figure 2.13: Reconfigurable gripper for plastic part extraction proposed in [5]

and flexible solutions, in comparison to the problem to be addressed. The resulting solution is a reconfigurable gripper, which needs the intervention of a worker to be set up for each batch; a flexible solution would be much more expensive and complex, but would not require human intervention. The authors assert that for the particular case, involving batches of fifty thousand units, the higher cost and complexity are not justified and the required intervention time can be neglected.

2.6 Cardboard Box Depalletizing Robot Using Two-Surface Suction and Elastic Joint Mechanisms: Mechanism Proposal and Verification

The paper [6] proposes a solution to transfer cardboard boxes from a roll box pallet to a conveyor belt, accounting for the possible shift of the boxes' positions. A depalletizing robot is developed, composed by a main arm and a conveyor arm. The
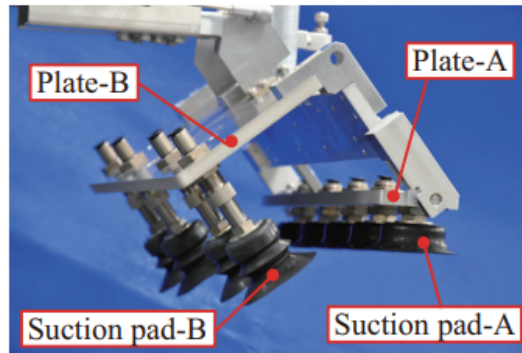
Figure 2.14: Developed end effector from [6]

main arm is equipped with an end effector, as shown in Fig. 2.14. It is characterized by two sets of suction cups, to contact the boxes on two surfaces; plate B uses spring-loaded cups, differing from plate A, each suction cup is connected to a pressure sensor and a switching valve, to control them individually. The end effector is attached to the main arm through an elastic joint, and can also rotate around the vertical axes (see Fig. 2.14), moved by pneumatic cylinders. The main arm has two linear actuators to perform a rough positioning, while the conveyor arm is equipped with a conveyor belt. The authors propose a transfer method divided into the following operations (Fig. 2.15):

- approach of the box from above using linear actuator of the main arm;

- use of the vacuum to hold the top and front surfaces of the box;

- lift of the main arm with consequent rotation of the spring joint caused by the box weight;

- position of the conveyor arm under the lifted box and activation of the belt;

- the box is placed on the belt moving the linear actuator of the main arm in the direction of movement of the belt;

- separation of the box from the end effector, and movement of the conveyor.

The solution of the two contact surfaces is used to reduce the moment load on the suction cups. The tests performed on the robot show that the pivoting end
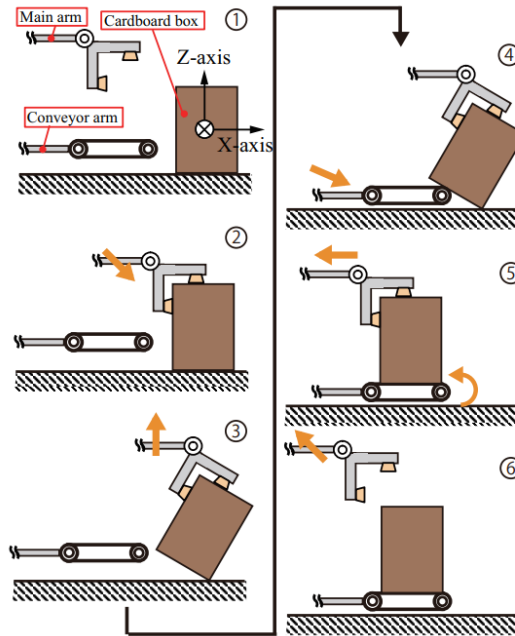
Figure 2.15: Proposed transfer method from [6]

effector is a valid solution since with a simple motion of the linear main arm, it is still possible to withstand the change in posture of the boxes.

Chapter 3

Problem definition

The following chapter focuses on the description of the addressed problem. The working objects and their layout are presented as indicated by the company. According to these specifications, the preliminary design choices are made and reported.

3.1   List of working pieces

Comau provided a list of various objects that will be handled in a depalletizing operation; the list is composed by ten lines, each line is assigned to a letter, for all of them different specifications are given:

- Goods in a Box: specifies the number of objects contained in each secondary packaging;

- Product Dimensions: specifies the dimensions of each object;

- Good weight: expresses the mass given in grams for each object;

- Box Dimension: gives the dimensions of the primary packaging;

- Net Box weight: gives the mass of each primary packaging expressed in grams;

- Boxes on a pallet: provides the number of primary packages in each pallet.

LINE	Goods in a Box	Product Dim	Good weight [g]	Box Dim	NET Box weight [g]	Boxes on a pallet EUR 1 (1200 x 800)
LINE A	10	128x72.5x148	566	148x256x362.5	5660	81
LINE B	12	101.5x101.5x118	505	304x406x118	6060	66
LINE C	400	142x60x9	16 (14.2)	250x400x300	5680	36
LINE D	400	140x60x10	26	250x400x300	6400	36
LINE E	12	95x95x390	353	465x375x394	448	18*
LINE F	96	90x31.5x120	79.7	378x360x240	6720	30
LINE G	24	130x90x130	271	390x260x360	6504	30
LINE H	6	99x63x145	177	145x99x378	1062	216
LINE I	12	281x37x38	81.5	281x111x152	978	232
LINE K	3	111x111x111	110	333x111x111	330	140 -208 -360

Figure 3.1: table of all the lines with specifications

Table 3.1 reports all the data.

3.2 Packaging layouts

As can be seen from Table 3.1, each packaging has different dimensions; this leads to a different number of objects for each line and also to a different layout. The company has provided also the different layouts for the lines.

Line A

Line A has two different layouts depending on the pallet dimensions, shown in Figs. 3.2 and 3.3.
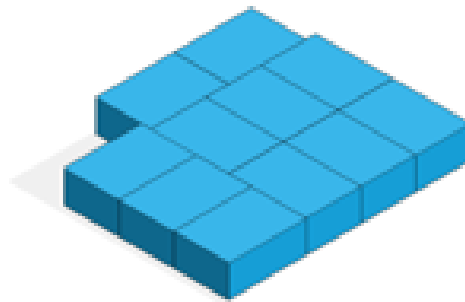
Figure 3.2: A layout with 1200x1000 pallet and 9 layers

16
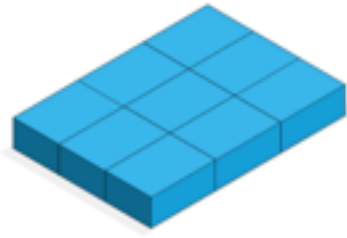
Figure 3.3: A layout with 1200x800 pallet and 9 layers

Line B

Line B has two different layouts depending on the pallet dimensions, shown in Figs 3.4 and 3.5.
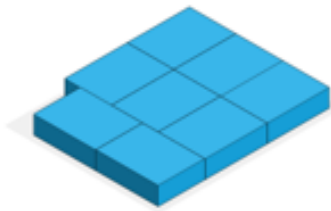
Figure 3.4: B layout with 1200x1000 pallet and 11 layers
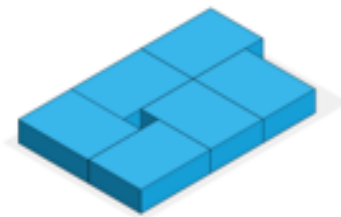
Figure 3.5: B layout with 1200x800 pallet and 11 layers

Line C

Similarly to line E, lines C and D have nine boxes per layer with four layers.

Line E

Line E has one possible layout, reported in Fig 3.6.
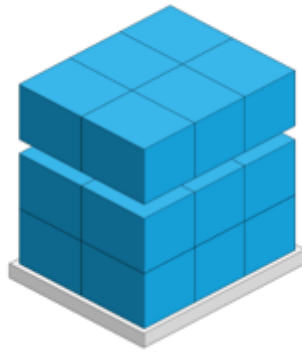
Figure 3.6: E layout with 1200x1000 pallet and 3 layers

Line F

Line F has one possible layout, it is shown in Fig. 3.7.
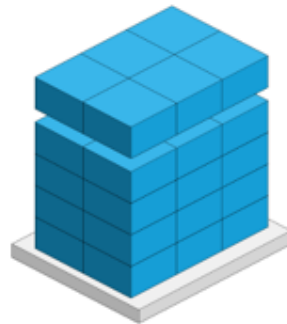
Figure 3.7: F layout with 1200x1000 pallet and 5 layers

Line G

Line G has one possible layout for both 1200x1000 and 1200x800 pallets, shown in Fig. 3.8.
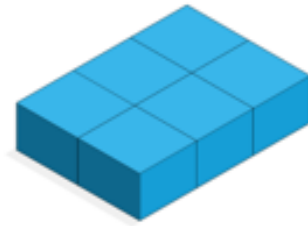
Figure 3.8: G layout with 1200x1000, 1200x800 pallet and 5 layers

Line H

Line H has two different layouts depending on the pallet dimensions, they are shown in Figs. 3.9 and 3.10.
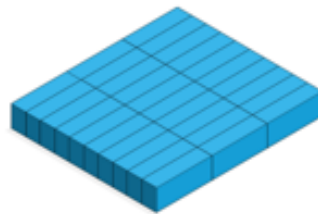
Figure 3.9: H layout with 1200x1000 pallet and 9 layers
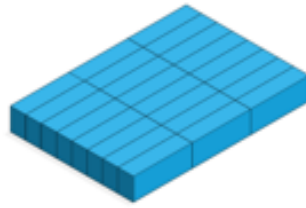
Figure 3.10: H layout with 1200x800 pallet and 9 layers

Line I

Line I has different layouts: three for the biggest pallet, reported in Fig. 3.11 and twelve for the smallest one, one of them is reported in Fig. 3.12.
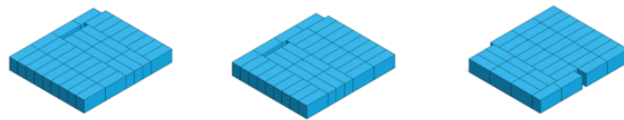
Figure 3.11: I layouts with 1200x1000 pallet and 8 layers
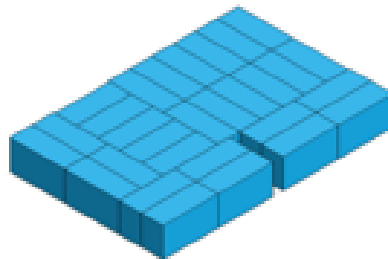
Figure 3.12: Example of I layout with 1200x800 pallet and 8 layers

Line K

Line K has one possible layout for the 1200x1000 pallet, reported in Fig. 3.13.
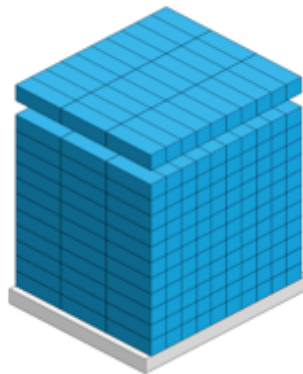
Figure 3.13: K layout with 1200x1000 pallet and 12 layers

3.3   Basic working principle definition

Analyzing all the lines, in particular the dimensions of the various boxes, it is clear that the gripper will need some degree of adaptability to the various lengths or widths of the boxes. As analyzed in the previous chapters, a gripper can be reconfigurable or also flexible. In [5] the authors choose to use a reconfigurable gripper, with the intervention of a human for positioning the suction cups; in this case a flexible solution, capable of adapting by itself, can be preferable, considering the big variability of the box dimensions and the fact that this is not a batch production. There are different options to provide some adaptability to the gripper: it is possible to find in the market some solution that provides this property equipping the gripper with multiple suction cups and controlling which of them is active to match the available area of the object to be grasped; the downside of this solution is the fixed maximum amount of suction cups available, and also the fact that for smaller objects some suction cups are not active, thus wasted. A more suitable solution could be one of the type studied in [4], where the suction cups are moved by a mechanism to adapt to different working objects; this solution provides a lateral grasp on the object, but the basic principle could be developed to match this study case. The final solution consists of a vacuum gripper with two degrees of freedom: the gripper is equipped with two rows of suction cups, their distance can be varied thanks to an electric actuation, the rows of suction cups are always parallel to each other. Moreover, since they are composed of simple extruded profiles to which the suction cups are attached, the layout and the number of suction cups can be varied according to the operation to be performed; the other degree of freedom is controlled acting on the active suction cups, this means that the gripper has different vacuum zones that can be activated or deactivated independently: for bigger or heavier object more suction cups can be used, but also the opposite can be done. The choice to develop a vacuum solution is motivated by the arrangement of the boxes in the pallet; since there is no space around them, they have to be lifted by their top side, which can be done by suction cups. Ejectors are employed to produce vacuum since they do not require additional parts, such as electric motors in the case of vacuum pumps. They can also ensure continuous air evacuation, unlike the pumpless devices discussed in [1]. Given the regular shape of the handled objects and the absence of height differences, flat suction cups are used. The proposed solution has to be defined at different levels:

- Mechanical Design: all the components, both commercially available or to be manufactured have to be defined; this is done using the software SolidWorks, in this way it is possible to create a virtual model of the gripper in an assembly, create the custom components, and test some component by means of a FEA;

- Pneumatic Design: since the gripper uses vacuum technology, it is necessary

to define all the components regarding the vacuum generation, the tubing, valves, suction cups, and all the supports; this phase is done focusing on the directives of the manufacturer of the various components;

- Electric Design: it is necessary to fix an architecture for all the electric and electronic components such as the various sensors, the actuator, and the motor controller;

- Control Architecture Design: finally, the way of controlling the gripper and interfacing it with the robot has to be defined.

In the following chapters, the design phases of the gripper are treated.

Chapter 4

Vacuum design

4.1 Basic principle of vacuum technology

As explained in [1], there are many ways and technologies to grasp an object using compressed air; one of them is to create a vacuum on the surface of the working object to generate a lifting force, this vacuum is usually pulled by a Venturi Ejector. The lifting force is given by:

$$F = P * A \tag{4.1}$$

where P is the pressure inside the suction cup and A is its active area. Depending on the working object, the pressure required to generate the lifting force changes, so it is necessary to analyze all the cases to set values, such as the required pressure, the characteristics, and number of the suction cups. Regarding the ready-to-buy components, it is chosen to use products by Festo, which is a leading company in the field

4.2 Suction cups and vacuum zones

To define the number, dimensions, and material of the suction cups, it is fundamental to look at the objects to be grasped. In this case, all the objects consist of secondary packaging. They are assumed to be made of the same kind of cardboard and to have a uniform distribution of the weight. The mass of the box has to be converted into a holding force, which is the force that the suction cup or cups should exert on the object to hold it during the movement. Festo proposes its procedure to compute the holding force depending on the direction of the movement and the orientation of the suction cup.

- In case 1, shown in Fig. 4.1, the suction cup is horizontal, and the direction of the movement coincides with the symmetry axis of the cup itself; this represents, when considering equal condition, the less stressful movement for the cup. The holding force is given by:

$$F_H = m * (g + a) * S \tag{4.2}$$

- In case 2, shown in Fig. 4.2, the suction cup is horizontal, the direction of the movement is also horizontal, so in the same plane defined by the contact area between the cup and the piece. This case is more demanding on the suction cups: the nature of the movement makes the friction between the cup and the object arise as a scaling factor for the acceleration. The holding force is given by:

$$F_H = m * (g + a/\mu) * S \tag{4.3}$$

- In case 3, shown in Fig. 4.3, the suction cup is vertical, and the direction of the movement is also vertical; this situation requires the biggest holding force:

$$F_H = m/\mu * (g + a) * S \tag{4.4}$$
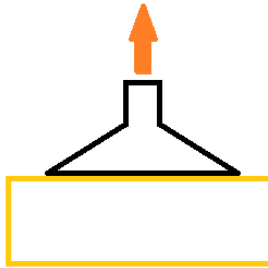
Figure 4.1: Movement 1

The variables in (4.2)-(4.4) are defined as follows:

- F_H is the theoretical holding force required by the movement of the object expressed in Newtons [N];

- m is the mass of the working object;

- g is the gravity acceleration;

- a is the acceleration of the system which, in this case, is equal to 2 g;
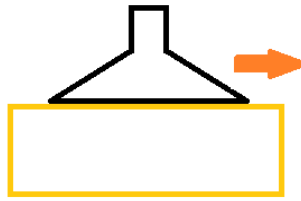
Figure 4.2: Movement 2
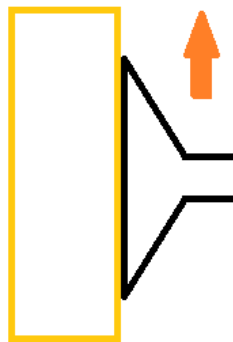
Figure 4.3: Movement 3

- S is the safety factor which is considered equal to 2 according to the rough surfaces involved, as requested by the Festo guidelines;

- μ is the friction factor, which in the case of rough surfaces is equal to 0.6.

All the theoretical holding forces are reported in Tab. 4.1. Since the last case requires the biggest holding forces, it will be used to dimension the vacuum system, taken as the worst scenario. It is decided to use a total of ten suction cups distributed on two extruded profiles, whose relative distance can be varied. A higher number of suction cups, in general, leads to a lower necessary level of vacuum, given the higher active area, as can be seen in (4.1). A simple solution could be represented by the direct connection between the suction cups and the vacuum generator, the downside is represented by the vulnerability of this method: a decompression in any of the suction cups could cause the loss of the vacuum in the whole circuit and the consequent fail of grasping. To avoid this problem a multi-zone system can be used; this solution requires the presence of different

		Theoretical holding force [N]		
Line	Box Weight [kg]	Case 1	Case 2	Case 3
A	5,66	333,1	481,2	555,2
B	6,06	356,7	515,2	594,5
C	5,68	334,3	482,9	557,2
D	6,5	382,6	552,6	637,7
E	0,448	26,4	38,1	43,9
F	6,72	395,5	571,3	659,2
G	6,504	382,8	553,0	638,0
H	1,062	62,5	90,3	104,2
I	0,978	57,6	83,1	95,9
K	0,33	19,4	28,1	32,4

Table 4.1: Theoretical holding forces depending on the type of movement and the weight of the box

vacuum generators attached to a limited number of suction cups, in this way the loss of pressure in one of the circuits does not propagate to the other. This solution provides redundancy to the gripper, but can also lead to a reduction in the consumption of air, since the cups that are not in contact with the piece can be turned off. Analyzing the different kinds of boxes to be grasped, it is chosen to use three different vacuum zones:

- a first central zone consisting of three suction cups mounted on the same extruded profile;

- a second central zone consisting of three suction cups mounted on the opposite extruded profile;

- another zone consisting of four suction cups mounted on both the extruded profiles;

The zones division is represented in Fig. 4.4, where each of them has a different color. With these vacuum zones, there can be several kinds of grasp depending on the box dimensions:

- for large boxes, all the vacuum zones can be activated to provide redundancy and a more stable grasping, as shown in Fig. 4.5;

- for narrow boxes, it is possible to use the inner zones only or all of them to have redundancy, or one of the inner ones to grasp only one box, as shown in Fig. 4.6;

27
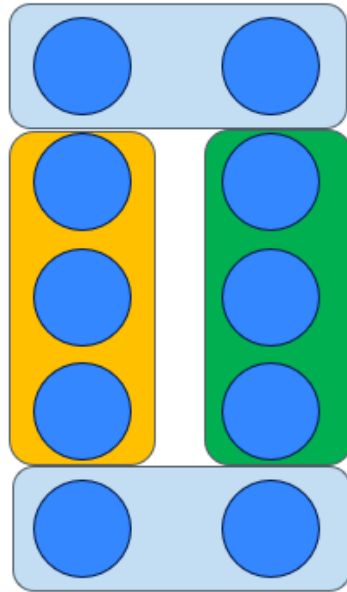
Figure 4.4: The three vacuum zones represented in different colors

- for narrow and short boxes, the inner zones are used, one of them or both according to the number of boxes to grasp, as can be seen in Fig. 4.7.
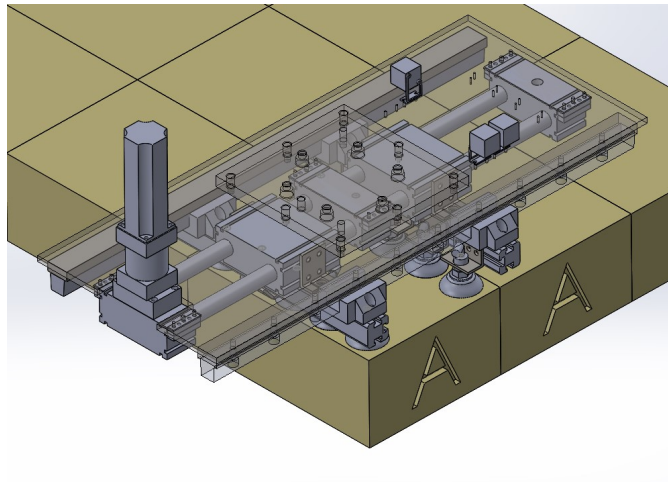
Figure 4.5: Grasping of large boxes (A line)
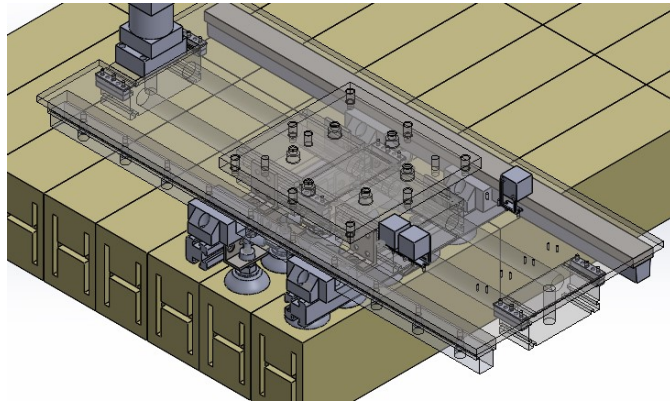
Figure 4.6: Grasping of narrow boxes (H line)
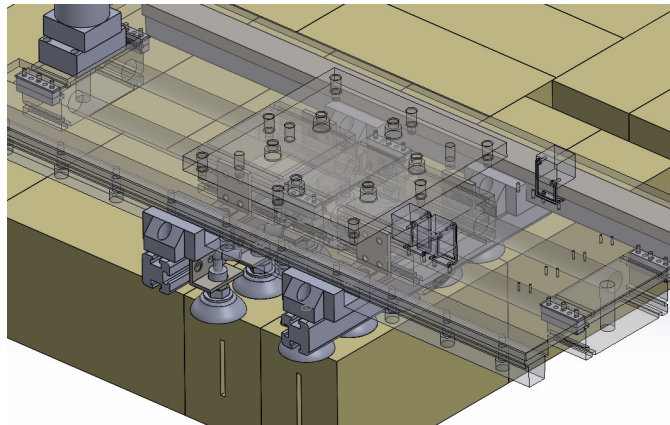
Figure 4.7: Grasping of narrow and short boxes (I line)

Once the number of suction cups to use and the theoretical holding forces are known, the model of the suction cup can be chosen. It is necessary to find which are the required forces to be provided by the suction cups depending on the grasp scenario; as explained before, the same box can be grasped using a different number of cups. For example, considering the case of a single vacuum zone failure, Tab. 4.2 shows necessary forces according to the number of active cups; for the last three lines the theoretical force is doubled, since it is considered to grasp two boxes simultaneously:

- the first column shows the forces in the case of contact of all the suction cups; it is available only for the bigger boxes;

- the second gives the value when using only the two inner zones; it is available for all the boxes;

- the last gives the value obtained when using one of the inner zones, and the outer one; it is not available for the smaller boxes because when only one item is grasped the outer zone loses its vacuum.

		Single cup necessary holding force [N]		
LINE	Th. Force [N]	Active cups number		
		10	6	7
A	555,2	55,5	92,5	79,3
B	594,5	59,4	99,1	84,9
C	557,2	55,7	92,9	79,6
D	637,7	63,8	106,3	91,1
E	43,9	4,4	7,3	6,3
F	659,2	65,9	109,9	94,2
G	638,0	63,8	106,3	91,1
H	208,4	20,8	34,7	
I	191,9		32,0	
K	64,7		10,8	

Table 4.2: Theoretical holding force for different numbers of suction cups

The values are calculated simply as follows:

$$F = F_H/n \tag{4.5}$$

where F_H is the previously computed theoretical force and n is the number of active cups considered. Choosing a suction cup with a diameter of $60mm$, it is possible to compute the active area as:

$$A = \pi * d^2/4 = 0.0028m^2 \tag{4.6}$$

Dividing the previously found theoretical holding force by this area it is possible to find the required pressure; all the values are reported in Tab. 4.3. Analyzing the obtained value, a minimum vacuum level of $P = -0.4bar$ is used as the desired value. Taking into consideration the maximum theoretical force that an individual cup shall provide, it is chosen to use a suction cup by Festo, model ESS-60-SU, (shown in Fig. 4.8), which has a diameter of $60mm$. It can produce a lifting force of $166.1N$ at $-0.7bar$ and it is made of polyurethane, which gives a good resistance to wear and abrasion.

LINE	Th. Force [N]	Required pressure [bar relative]		
		Active Cups number		
		10	6	7
A	555,2	0,20	0,33	0,28
B	594,5	0,21	0,35	0,30
C	557,2	0,20	0,33	0,28
D	637,7	0,23	0,38	0,32
E	43,9	0,02	0,03	0,02
F	659,2	0,23	0,39	0,33
G	638,0	0,23	0,38	0,32
H	208,4	0,07	0,12	
I	191,9		0,11	
K	64,7		0,04	

Table 4.3: Required pressure for different numbers of suction cups

Figure 4.8: Festo ESS-60-SU

4.3   Suction cups mountings

The selected suction cup has a vacuum $M10$ threaded male connection. To mount the cup on the extruded profile, it is necessary to use another component, which is a suction cup holder, specifically the model ESH-HA-5-G by Festo; it has a $M10$ mounting for the suction cup, a $G1/8$ threaded connection for the vacuum circuit, and can be fixed on a hole by two locking nuts (Fig. 4.9).

On top of the latter is is mounted an L-shaped push-in fitting, Festo QSL-G1/8-6 which provides a quick mount for a tube with an external diameter of $6mm$ (Fig. 4.10).

31

Figure 4.9: Festo ESH-HA-5-G

Figure 4.10: Festo QSL-G1/8-6

4.4 Vacuum distribution

It is necessary to connect together some of the cups in order to obtain the previously explained vacuum zones; this is done with multiple distributors, which have one intake and several output ports. In this particular case, two kinds of distributors are needed: one with three outputs for the central zones and one with four outputs for the outer zone. It is chosen to use a Festo QSLV3-1/4-6 (Fig. 4.12), and a Festo QSQ-G1/4-6 (Fig. 4.11), the out-ports of these components have a quick mount for the tube, the intake is a threaded connection $G1/4$ or $R1/4$; to the latter, it is attached an adapter that gives on the other port again a quick attachment for the tube, this is a Festo QSF-1/4-6 (Fig. 4.13).

Figure 4.11: Festo QSQ-G1/4-6

Figure 4.12: Festo QSLV3-1/4-6

Figure 4.13: Festo QSF-1/4-6-B

4.4.1 Volume estimation

A crucial factor is the volume of air to be evacuated in each vacuum zone. To estimate this value it is possible to sum the volumes of all the single parts present in the circuit and add the volume of the tubes with an estimated length. All the volumes, if available, are taken from the component manufacturer; all the components with an available volume value are now listed together with the value.

- Festo ESH-HA-5-G, $V = 1.862cm^3$;

- Festo ESS-60-SU, $V = 3.953cm^3$;

A big contribute to the total volume comes from the tubing; in this case, the used tube is a PUR tube with an outer diameter of $6mm$, and an inner diameter of $4mm$. The inner diameter is used to calculate the section of the tube; the tube volume is then given by:

$$V = \pi * d_{in}^2/4 * L \tag{4.7}$$

where L is the estimated length of the tube. The path is estimated in the following way. The tubing starts from one of the short sides of the gripper and reaches the middle of the gripper length. From this point, the tubing is split according to the number of suction cups to be reached. The hoses then go to the opposite side of the gripper and back toward the starting point. The path of

33

the tubes for the three cups zone is shown in Fig. 4.14, along with the assumed dimension.

Figure 4.14: Conservative tubes path for 3 cups channel

The lengths are computed as follows:

$$L_3 = l_{min}/2 + l_{max}/2 + 3*(l_{min} + l_{max}/2) = 2933mm \tag{4.8}$$

$$L_4 = l_{min}/2 + l_{max}/2 + 2*(l_{min} + l_{max}/2) + 2*l_{max}/2 = 2995mm \tag{4.9}$$

The value of $2995mm$ is considered, increased by a factor of 20% giving a tubing volume:

$$V = \pi * d_{in}^2/4 * L * 1.2 = 45163.5mm^3 \approx 0.045l \tag{4.10}$$

Adding the known volumes for the other components in the circuit previously listed, the following volume is obtained for the four cups zone:

$$V_4 = V + 4*(0.002 + 0.004) = 0.069l \tag{4.11}$$

Considering the uncertainty on the other components, which are not provided of a volume specification, and the variability of the tubes path, it is considered to have a volume to be evacuated of $0.1l$.

4.5 Vacuum generation and sensors

The last part regarding the vacuum design consists in the definition of the vacuum generators to be used and the components to monitor the vacuum in the system. Among all the different generators available on the market, the focus is toward the model which can be enabled by an electric signal; Festo provides a family of vacuum generators, called *VN* which is also available in a variant provided with a solenoid

valve that can be turned on or off to toggle vacuum generation. This variant is denoted by an *M* in the product name. This class of generators is available with different Laval nozzle sizes; this factor determines the performance of the generator in terms of suction rate, which is the volume of air pulled from the atmosphere, maximum vacuum level, and in particular evacuation time and air consumption. To select a suitable vacuum generator for the specific application, all the available variants with their specification are put in the Tables 4.4 and 4.5 to perform a comparison. Pressure values regarding P_u are expressed without a minus sign, but they represent a negative pressure relative to the atmosphere.

Entries	P_1[bar] to obtain $P_u = 0.4bar$	P_u at $P_1 = 6bar$	P_u at $P_1 = 4bar$	Evacuation time [s] at $P_u = 0.4bar$ for 1*l* with $P_1 = 6bar$	Suction rate[l/min] from atmosphere vs at $P_{1,0.4}$
VN-05-H	1,7	0,9	0,9	4	7
VN-07-H	2	0,9	0,9	1	16
VN-10-H	2	0,9	0,92	1	19
VN-14-H	2	0,89	0,9	0,5	48
VN-20-H	2	0,89	0,9	0,25	100
VN-30-H	2	0,92	0,92	0,15	155
VN-05-L	2,5	0,75	0,6	2	11
VN-07-L	2,6	0,77	0,6	1	26
VN-10-L	2,5	0,87	0,7	0,5	32
VN-14-L	3	0,9	0,56	0,25	80

Table 4.4: Vacuum generator comparison 1

Entries	Suction rate [l/min] from atmosphere at $P_1 = 6bar$	Suction rate [l/min] from atmosphere at $P_1 = 4bar$	Air consumption q_n [l/min] at $P_{1,0.4}$	Air consumption q_n [l/min] at $P_1 = 4bar$
VN-05-H	7	7,5	5	9
VN-07-H	15	16	12	20
VN-10-H	19	20	22	39
VN-14-H	44	48	50	90
VN-20-H	92	100	100	180
VN-30-H	172	180	200	340
VN-05-L	14	13		
VN-07-L	29	28		
VN-10-L	40	40		
VN-14-L	89	90		

Table 4.5: Vacuum generator comparison 2

Each row of the table corresponds to a variant of generator, the number indicates the nozzle size, the letter *H* stands for standard generator or high vacuum, the letter *L* stands for high suction rate model. All the columns provide the characteristics of the ejector as reported in the diagrams that can be found in the product datasheet:

- The first column shows the required intake pressure P_1 to obtain the desired pressure $P_u = -0.4bar$, which is the minimum vacuum value required in the

considered application; in this case, a lower value indicates a less demanding generator.

- The second column shows the pressure generated by the ejector P_u, when a pressure $P_1 = 6bar$ is applied, denoting the maximum performances of the generator.

- The third column gives the pressure P_u when a $P_1 = 4bar$ is applied; this particular intake pressure is the pressure usually available from the plant as indicated by Comau (in this case, high values are better).

- The fourth column gives the evacuation time in seconds, for a volume of $1l$ at an operating pressure $P_1 = 6bar$; a low value is desirable.

- The fifth, sixth, and seventh columns express the suction rate in l/min of air from the atmosphere at different operating pressure: the first is the $P_{1,0.4}$ extracted from the first column, the second is $P_1 = 6bar$ and the third is $P_1 = 4bar$.

- The last two columns give the air consumption as l/min at the P_1 given by the first column and at $4bar$.

The table shows that bigger nozzle sizes provide much shorter evacuation times and higher suction rates, but this is possible only with a bigger air consumption. Given the previously calculated volume of air to be extracted, which results to be small, one of the smaller vacuum generators can be chosen; in particular, the model Festo VN-07-H-T3-PQ2-VQ2-RO1-M is selected, which could evacuate the volume in the following time:

$$t_s = E_t * V = 1 * 0.1 = 0.1s \tag{4.12}$$

where $E_t = 1$ is the evacuation time for one liter of air when working at $P1 = 6bar$. This ejector could produce the required vacuum operating with $P_1 = 2bar$, using $P_1 = 4bar$ as usually available in Comau applications, the produced vacuum is higher. Testing the components can show if such an operating pressure is suitable for cardboard boxes and to check the functionality of the whole system; assuming that the three generators work in the same conditions, the compressed air supply should provide:

- in the case of $P_1 = 2bar$, $q_n = 3 * 12 = 36l/min$ producing $P_u = 0.4bar$ in the cups;

- in the case of $P_1 = 4bar$, $q_n = 3 * 20 = 60l/min$ producing $P_u = 0.9bar$ in the cups;

Lastly, a component is chosen to have a feedback on the pressure in the system after the vacuum generators. The sensor is attached to the system through a push-in fitting as the other components, a T connector is necessary to split the vacuum line and reach the sensor as well as the suction cups. The sensor has a range between $-1bar$ and $1bar$, and can be configured to output a signal when a threshold pressure is reached. The sensor is the Festo model SPAN-B-B2R-Q4-PN-L1 shown in Fig. 4.15; the T shape adapter is a Festo QST-6-4 (Fig. 4.16) provided with two $6mm$ ports and one $4mm$ port.

Figure 4.15: Festo SPAN-B-B2R-Q4-PN-L1

Figure 4.16: Festo QST-6-4

Finally, a high-level schematics for the vacuum circuit is produced and reported in Figure 4.17; in the left side of the diagram the inlet for the pressurized air supply is represented. From the inlet the flow of air has to be distributed to the individual vacuum generators, which have a push-in fitting for tube with an outer diameter of $6mm$ (port 1). For each vacuum generator, the output port 2 is connected to the previously mentioned T-shaped distributor, where the vacuum sensor is also connected via a smaller tube, as well as the $6mm$ tube for the connection with the distributors QSF-1/4-6 or QSLV-1/4-6 depending on the number of cups. After the distributor, the various suction cups are connected via $6mm$ outer diameter tube.
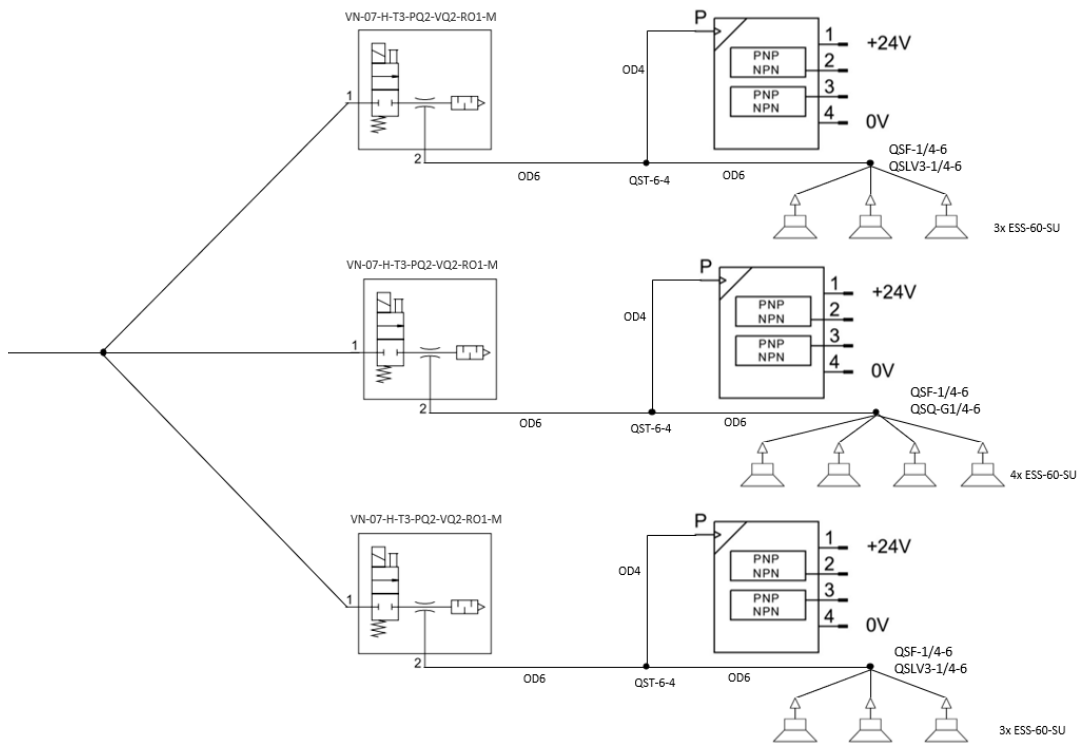
Figure 4.17: Pneumatic circuit diagram

Chapter 5

Mechanical design

In the following chapter, the process of the designing phase is shown in terms of standard components selection and design of custom parts. The final goal of this chapter is to show the produced 3D mock-up of the gripper, provide detailed information about all the components of the product, and about the static analysis conducted on them.

5.1 Utilized software

In this phase of the work the used software is SolidWorks 2022 produced by Dassault Systèmes. It is a computer-aided design or CAD software that provides all the tools for the realization of parts, assembly, and part drawings; moreover, using the SolidWorks Simulation package is possible to realize Finite Element Analysis, which are used to perform static analysis on the custom made components.

5.2 Starting considerations

In Chapter 3 the basic working principle desired for the gripper is explained, highlighting the need for a flexible product. Given the varying of the working pieces, the starting point for the mechanical definition is the determination of the dimensions of the main components. In Figure 5.1 a schematic view of the gripper is reported: the two vertical elements are the rows of suction cups, represented by blue circles, that should move closer or apart from one respect to the other; this particular characteristic is denoted by the dimension $L2$. The measure of the row itself, however, has to be chosen a priori, based on the particular working conditions: in the figure this feature is denoted as $L1$. To define the two main dimensions of the gripper, some trivial considerations are made, based on the case study. The analysis of the different kinds of boxes gives a minimum value
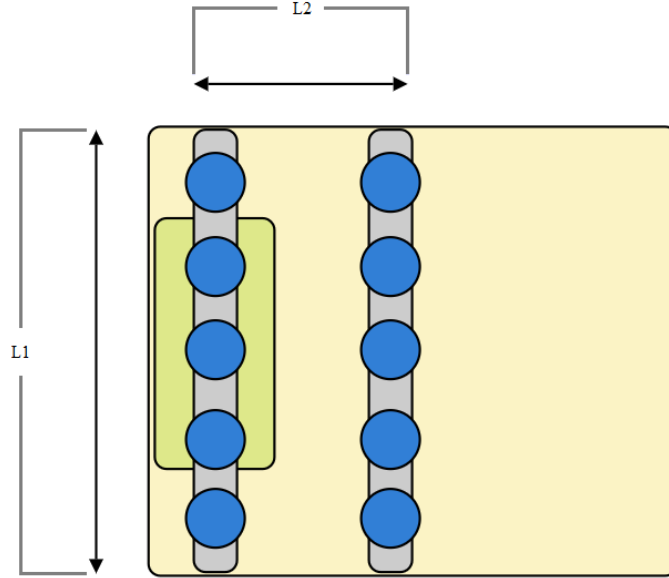
Figure 5.1: Preliminary dimensions selection

for the two elements: as can be seen from Fig. 5.1 in the background two boxes are represented in green and yellow, (the drawing are not in scale); it is assumed that the gripper will contact the boxes as shown in the image, so with the rows of suction cups parallel to the biggest dimension of the box, while the smallest dimension will be covered by the movement of the rows. It is now clear that the dimension $L1$ it has to be shorter than the biggest of the boxes, so

$$L1 <= length_{lineE} = 465mm \tag{5.1}$$

Instead, $L2$ should be bigger than the narrowest box, so

$$L2 >= width_{lineH} = 99mm \tag{5.2}$$

These values are only taken as a starting point; in the next chapters the actual capabilities of the gripper will be shown and the choices will be explained. Regarding the movement of the suction cup rows, it is intended to find an actuator that can move both of them at the same time, with an opposite movement and utilizing the minimum number of motors.

5.3   Suction cup rows actuator

To achieve the desired movement, it is necessary to evaluate the available solutions on the market. Many manufacturers produce different kinds of actuators; the main types are rotary and linear actuators, these elements can be based on different working principles, the main being pneumatic or electric. For the gripper under study, it is chosen to have an electric actuator, to have a simple positioning control to be performed by the motor drive itself. Among the electric actuators, manufacturers such as Festo propose a variety of electric axes, which are components suitable for linear motion. They can be belt-driven or screw driven. When looking for a solution that provides a reciprocating movement the options merge to a belt-driven electric axis, in particular, the product family is Festo ELGG. The axis is composed of a support structure made of two cylindrical rails on which two slides can move; it has three mounting blocks: two are placed at the extremities of the rails and one in the middle. The axis is sold without any electric motor, but it can be mounted in four different positions; moreover, the presence of various grooves makes easy the mounting of the axis to a base and of the other elements to the slide. Figure 5.2 shows a basic configuration of the axis. The selected electric axis is available in

Figure 5.2: Festo ELGG belt driven electric axis from Festo website

different sizes, characterized by three different thickness values of the component: $35mm$, $45mm$ and $55mm$. Bigger sizes give different characteristics as shown in Table 5.1.

As it will be later explained, the axis will only provide a push-pull force to the suction cup rows, without any support function; this means that among all the listed features, the ones to be taken into consideration for the selection are the *Feed force*, the *Velocity* and the available working stroke. Regarding the velocity and the

Size	Working stroke per slide [mm]	Velocity [m/s]	Accuracy [mm]	Feed force [N]	$F_y[N]$	$F_z[N]$	$M_x[Nm]$	$M_y[Nm]$	$M_z[Nm]$
35	50-700	3	±0.1	50	50	50	2.5	20	20
45	50-900	3	±0.1	100	100	100	5	40	40
55	50-1200	3	±0.1	350	300	300	15	124	124

Table 5.1: ELGG axis characteristics

working stroke, all the variants of the product are suitable for the application. The feed force is the maximum load that can be applied on the two slides combined along the direction of movement, an estimation of this load is computed to select a suitable model. In Figure 5.3 a schematic representation of the axis is shown. As indicated by the Comau team the accelerations to be used as reference for the computation of the forces is $a = 2 * g$ where $g = 9.81 m/s^2$. In this case, it is assumed that during the movement of the gripper the accelerations shown in the figure are applied to the slides, the masses attached to the slides will be around $m = 3.5kg$, for the computation of the forces, it is assumed to have $m = 4kg$, thus obtaining:

$$F_{feedtotal} = 2 * m * a = 2 * 4 * 3 * 9.81 = 235.4N \qquad (5.3)$$

Note that the acceleration a is enlarged by one g assuming that the Earth's gravity adds to the acceleration of the slides. The resulting value, which is already computed as the resultant of the two slides, is suitable only with the biggest size of the electric axis, so the latter is selected for the mock-up. The working stroke for each slide of the axis is set to $200mm$, so the distance between the suction cup rows can be set from $90mm$ to $520mm$.
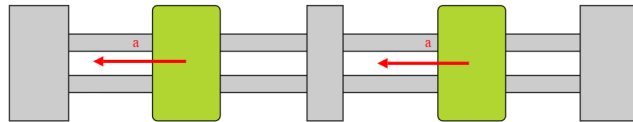
Figure 5.3: Accelerations acting on the slides

5.3.1 Motor selection and mounting

To select the electric motor to use, it is considered to have an available torque that can reach the maximum feed force of the axis. The electric axes can be equipped with a servo motor or a stepper motor; to select the motor model, it is necessary to define a torque requirement. To compute the needed torque, the diameter of the

pulleys inside the electric axis is used; it corresponds to $d = 28.65mm$, giving:

$$T = F_{feedmax} * d = 350 * 28.65/1000 = 10.03Nm \tag{5.4}$$

The motor is mounted to the axis through a so-called *Mounting Kit*, plus, a gear reduction element can be added. It is chosen to utilize a Festo EMGA-60-P-G8-SST-57 as a gear reduction element, (Fig. 5.4); this is mounted on one side to the motor, and on the other to the mounting kit. The EMGA gives a 8:1 reduction ratio, this means that the torque provided by the motor is multiplied eight times, giving a lower rotational speed.
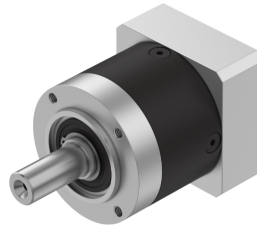
Figure 5.4: Festo EMGA-60-P-G8-SST-57 from Festo website

The required mounting kit should provide two interfaces: the R48 one to be mounted on the axis, and the dimension 60 one on the other to be mounted on the gear reduction; it is selected a Festo EAMM-A-R48-60G (Fig. 5.5).

Figure 5.5: Festo EAMM-A-R48-60G from Festo website

For the motor selection, the required torque is evaluated, knowing that the torque provided by it will be enlarged by the reduction gear. A stepper motor

by Festo is selected, model EMMS-ST-57-M-SEB-G2 5.6; it has a holding torque of $T = 1.4Nm$ and can reach $1740rpm$, this variant has an internal encoder and works with a tension of $V = 24VDC$.

Figure 5.6: Festo EMMS-ST-57-M-SEB-G2 from Festo website

It is now possible to compute the available torque and the resulting linear speed of the axis as:

$$T_{res} = T_{mot} * r * \eta = 1.4 * 8 * 95/100 = 10.64Nm \tag{5.5}$$

where T_res is the resulting torque transmittable to the axis, r is the gear reduction ratio and η is the efficiency of the reduction. The maximum linear velocity of the axis is computed as:

$$v_{max} = \omega_{max}/r * d/2 = 1740 * 1/8 * 28.65/(2 * 1000)/60 = 0.052m/s \tag{5.6}$$

where v_{max} is the theoretical maximum linear velocity of the slides, ω is the maximum rotational speed of the motor, r is the reduction ratio and d is the diameter of the pulley previously introduced. The stroke of $l = 200mm$ can be run in $t = l/v_{max} = 3.85s$

5.4   Suction cups row

In the previous chapters, the selection of the vacuum element was explained, particularly one of the main components of the gripper is the suction cup unit, composed of several elements. In the proposed solution the suction cups have to be mounted on a component so to let all of them move simultaneously. The gripper has two moving rows of suction cups. All the suction cup units have to be mounted on a main support element, which has also to be coupled to the slides of the electric axis, as well as some support components. Keeping in mind that the

utilization of standard components is preferred, it is chosen to exploit an extruded profile by BOSCH; the particular model is 40x40L-3N,(Fig. 5.7). The extruded profile has a length of $400mm$, chosen for the case under study, but the measure could be modified to accommodate for more cups or more spacing between them. Figure 5.8 shows the main characteristics of the extruded profile; the groves are
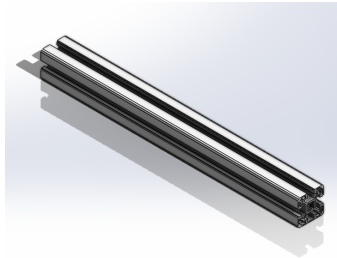
Figure 5.7: BOSCH 40x40L-3N extruded profile
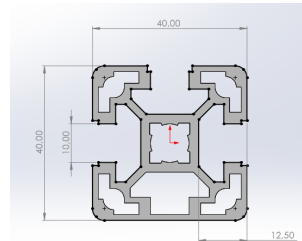
Figure 5.8: Extruded profile main dimensions

used for mounting other elements using a hammerhead nut. The suction cup unit has a pass-through mounting composed of two nuts screwed on the main body of the component, the nuts are used to clamp the piece in a hole. To mount all the suction cup units on the extruded profile, a custom piece is modeled through SolidWorks; the component is an L-shaped mount that presents the holes for both the connection of the suction cup holder and for the assembly to the profile. Fig. 5.9 shows the modeled component: it has three holes on one surface, the biggest is a through hole for an M8 screw, the others are meant to be the mounts for a positioning pin; the biggest hole is designed for the Festo ESH mount.
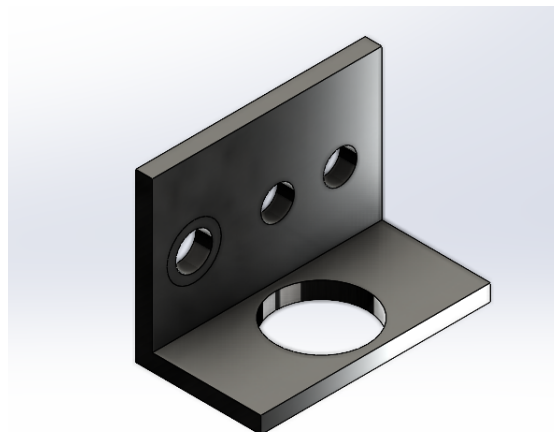
Figure 5.9: L-shaped suction cup unit holder

Fig. 5.10 reports the drawing for the component; the thickness of the components is *4mm*, and the dimensions are selected so to obtain a feasible assembly of the elements, such as nuts and screws.
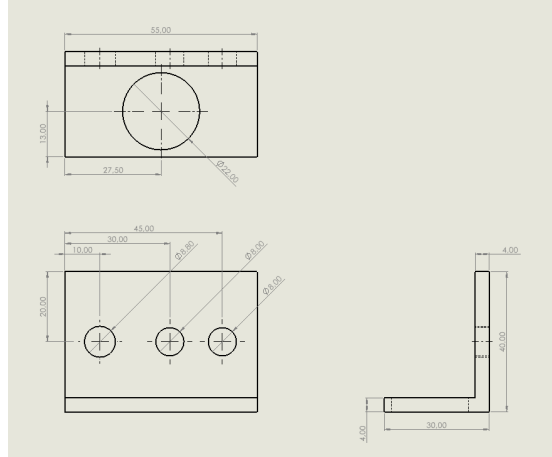
Figure 5.10: L-shaped holder drawing

It is chosen to perform a static analysis on the custom-modeled components, to see their behavior in a load condition, and check if they are suitable for the application. Solidworks offers the software Solidworks Simulation that can be used for static analysis, frequency studies, fatigue studies, and others. Solidworks Simulation uses the Finite Elements Method, which is a modelling technique based on the division of a system in many simpler elements, turning a complex problem into many simple problems. A single element is said tetrahedral element, composed of nodes and edges that can be straight or curved; it has some parameters that describe its state, and the results of an analysis are based on the interaction between the nodes. To perform a finite element analysis it is necessary to convert the model in a good-quality mesh and define the constraints and the loads that the model undergoes.

Figure 5.11 shows the model with all the applied constraints and loads, which are now explained in detail:

- to simulate the screw connection, the movement along the radial direction of the hole is blocked, and a constraint is applied to the annular surface surrounding the hole to block its movement along its normal direction;

- to the back surface of the object is applied a virtual wall constraint, which simulates the presence of a wall; in this case, it would be the extruded profile;

- the hole on the right has a fixed constraint in the inner surface to simulate the presence of a positioning pin;

46
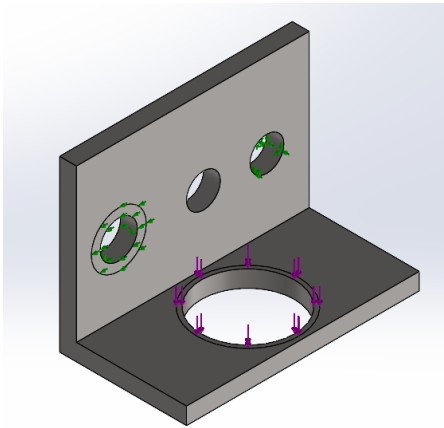
Figure 5.11: Loads and constraints applied to the model
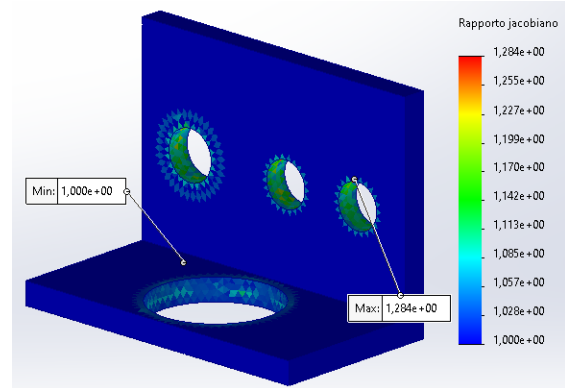
Figure 5.12: Mesh for the FEA analysis with jacobian ratio

- the load is applied to the annular surface surrounding the hole for the suction cup mount; it corresponds to the area where the suction cup mount is fixed, the load is set to $F = 200N$ corresponding to the nominal force that a cup can produce enlarged by 20%.

The model of the component is then converted into a mesh. The mesh definition can be set from draft quality to high quality. In draft quality, the mesh is composed of linear tetrahedral solid elements composed of four nodes and six edges; in high quality, the mesh is composed by parabolic tetrahedral solid elements with additional six nodes in the middle of the edges. A high-quality mesh provides better results but requires more computation time. In this case, given the simple model, a high-quality mesh is used. According to the software indication, the quality of a mesh can be checked by looking at two parameters: the aspect ratio, and the Jacobian ratio. The first parameter is given by the ratio of the longest edge and the shortest normal going from a vertex to the opposite face for each tetrahedron; a good mesh should have this value lower than five for at least ninety percent of the elements. The second parameter is used for high-quality meshes, it gives information about the deviation of a tetrahedron from an ideal one with all straight edges. In this case a good mesh should have this value between one and ten for at least the ninety percent of the elements. Fig. 5.12 shows the resulting mesh and the superimposed jacobian ratio; the minimum value is 1 and the maximum is 1.284. The mesh details section specifies that the percentage of distorted element is zero and all the elements have a aspect ratio lower than three, indicating a good mesh.

Once all the conditions are established, it is possible to execute the study, and collect the results; in particular, the main characteristics to analyze are the stress

in the piece and its deformation. Figure 5.13 shows the distribution of the von Mises stress in the piece, the graduated scale on the right gives the actual value corresponding to the different colors, expressed in MPa. It is clear that the plastic limit of the material which is chosen to be steel S355JR is not reached. Figure 5.14 shows, instead, the resultant displacement of the piece, in a deformed view; also in this case, the values are very low. The FEA shows that the piece could withstand with no problem the hypothesized stress condition. Finally, all the suction cup
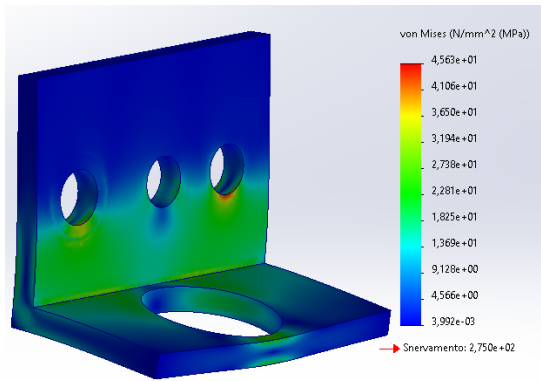
Figure 5.13: von Mises stress in the piece
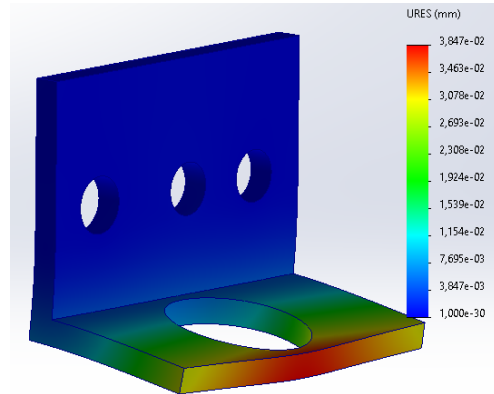
Figure 5.14: Resulting displacement of the component

units are assembled to the L-shaped holder and then all the holders are coupled with the extruded profile. The assembly is shown in Fig. 5.15; the holders are mounted on the profile using M8 screws and hammer head nuts placed into the profiles' groves.
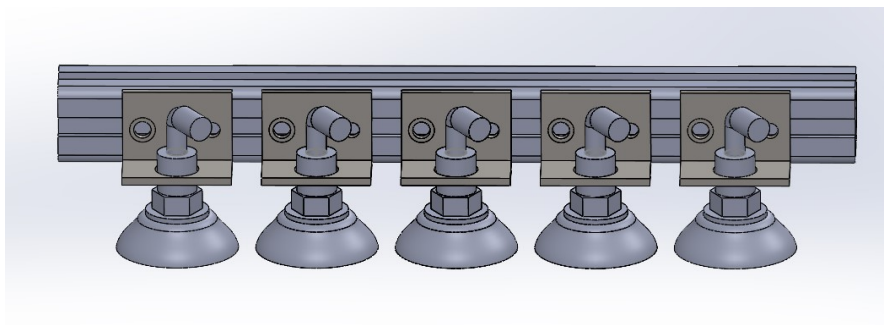
Figure 5.15: Assembly of one suction cup row

5.5 Main plate

To provide a basis framework for the gripper, it is chosen to model a simple plate. All the necessary components are mounted on this element, (see Figures 5.17 and 5.16).
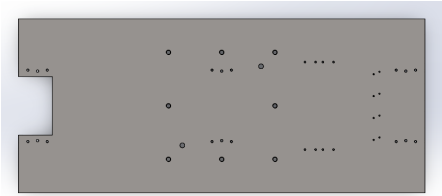
Figure 5.16: Top view of the main plate
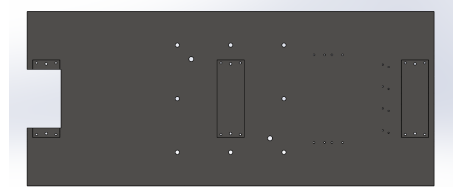
Figure 5.17: Bottom view of the main plate

The main function of the component is to provide the mounting points for the electric axes, with a precise and repeatable positioning; moreover, the plate is also designed to accommodate other elements, such as sensors, vacuum generators, and the adapter for the robot flange.

5.5.1 Axis mountings

To fix the electric axis on other components the particular design of its ends is exploited (see details in Fig. 5.18). Festo provides a mounting element called MUE45, which is composed of two parts: the first one is a basis that has to be mounted on the main component using two M5 screws, its positioning is fixed by a pin; the second part is screwed to the latter using two screws and has a hook shape that grabs into the axis end groves. In this case, the axis has two ends and one
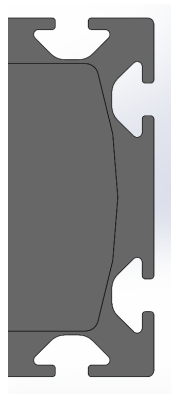
Figure 5.18: Side view of the groves on the axis ends and central support

central support. All these elements can be mounted using the MUE45 mounting elements. For the correct positioning of the axis on the plate, some particular choices are made: even if the MUE45 can fix the axis to the plate, this mounting does not guarantee the desired positioning; in particular, the axis has to be centered on the main plate. The MUE45, however, can grab into the grove of the blocks in every position, the mounting point is not referenced in any way, leading to a possible sliding of the axis ends. To fix this problem, the main plate has some recesses in which the ends of the axis and the center support have to be placed; they are two millimeters deep in the plate (a detailed view is reported in Fig. 5.19). For the mounting of the MUE45 basis, the plate has some threaded holes, along with a hole for a positioning pin; these are placed according to the MUE45 dimensions and positioning of the holes, in order to have a central positioning of the mounting element with respect to the parts of the axis to be fixed. The plate has a length of $840mm$ and a width of $358mm$, its thickness is $10mm$ and the selected material is steel S355JR; one of the smallest sides has a cut-out section, this is placed in the zone where the mounting kit and the rest of the motor assembly has to be placed.
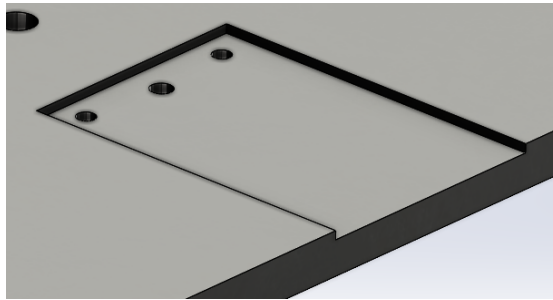
Figure 5.19: Section view of one of the recesses on the bottom side of the plate

5.5.2   Vacuum sensors and vacuum generator mounting

On the opposite side with respect to the motor mount area, there are some threaded holes for the connection of the vacuum sensors and the vacuum generator. These components are mounted to the main plate using particular elements, provided by the manufacturer:

- The vacuum sensors SPAN-B are mounted on a bracket model SAMH-PU-A via M3x8 screws, the bracket is assembled on the plate using M4 screws, the corresponding holes are the four pairs in the center-right part of the plate in Fig. 5.16;

- The vacuum generators are mounted on the VN-T3-BP brackets, which are screwed on the main plate via screws in the offset diagonally placed holes in

the right end of the plate in Fig. 5.16;

5.6   Support linear guides

The electric axis is only responsible for the movements of the suction cup rows, since the latter are not fixed to the slides of the axis. It is chosen to use some linear guide for the extruded profiles, which they can slide on. The selected models are produced by BOSCH Rexroth; the components are composed by a rail and a slide. In this case, it is chosen to use two slides per rail. The selected slide is the FKS R1665, which is suitable for medium load, the rail has a length of $820mm$ and is mounted using screws from the top (Fig. 5.20). The extruded profiles are mounted on the slides using M8 screws and a hammer nut placed in the profile groove; the screws are placed in the flanges of the slides from the bottom of Fig. 5.20. The rails are not directly assembled on the main plate: given the dimension

Figure 5.20: Linear guide from Bosch catalog

of the electric axis, a direct connection would not leave any space in the lower part of the gripper for the thickness of the ELGG-TB. The slide model is selected for its dimension and its flanges that allow the mounting on the extruded profiles. It is then necessary to compute a safety factor, considering the load applied. To estimate the load, it is assumed that the extruded profiles and the box are rigid; the loads are computed considering different directions of the acceleration applied to the box and the extruded profiles. Fig. 5.21 shows the load that can be applied to a single slide of the linear guide; the first load condition is reported in Fig. 5.22, where F_z is the load on a single slide, f_{row} is the force applied by one of the arm subject to the acceleration of $3g$, and C is the force applied by the box with the same acceleration. The force on the slide is computed as follows:

$$F_z = \frac{2 * f_{row} + C}{4} \tag{5.7}$$
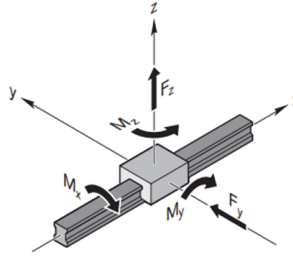
Figure 5.21: Possible loads on the slide

The second load condition is represented in Fig.5.23; the forces F_z on the slides
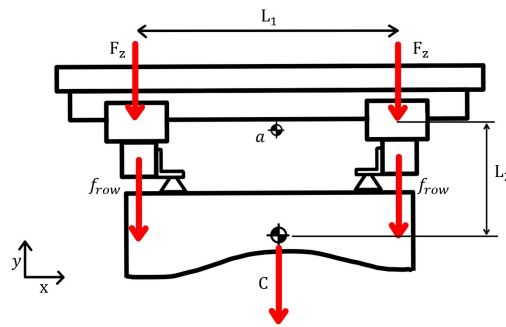
Figure 5.22: First load condition with -y acceleration

are equal in magnitude with opposite directions:

$$Fz = \frac{2 * f_{row} * L_4 + C * L_2}{2 * L_1} \tag{5.8}$$

where $L1$ is the distance of the slides along the rail, assumed to be equal to the box width, L_4 is the distance along y between the center of mass of the row, assumed to be in the middle of its height, and the center of the slide, and L_2 is the distance along y between the center of mass of the box and the center of the slide. The last load condition is shown in Fig.5.24. The resulting forces acting on the slides are computed:

$$F_z = \frac{2 * f_{row} * L_4 + C * L_2}{2 * L_3} \tag{5.9}$$

$$F_y = \frac{2 * f_{row} + C}{4} \tag{5.10}$$

The same forces are computed for each box; for the last case a combined load is computed as:

$$F_{comb} = |F_y| + |F_z| \tag{5.11}$$
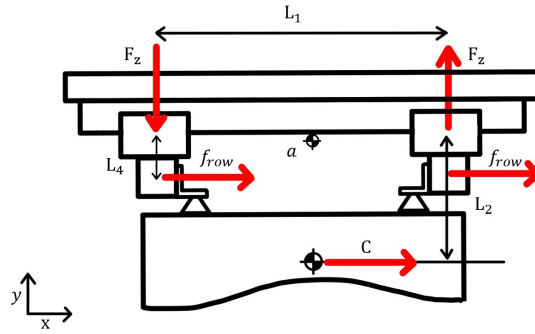
Figure 5.23: First load condition with x acceleration
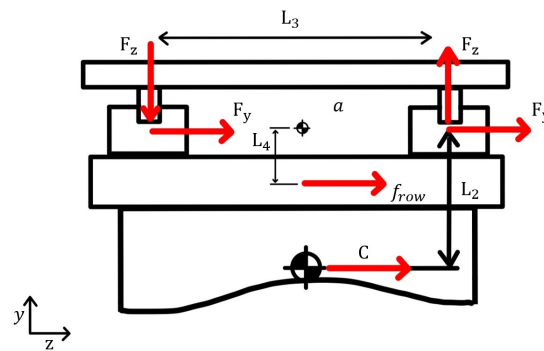
Figure 5.24: Third load condition with z acceleration

The maximum F_{comb} is used to compute a static safety factor as:

$$S_0 = \frac{C_0}{F_{0max}} = \frac{28900}{147} = 196.6 \qquad (5.12)$$

The safety factor S_0 should be greater than 12 in the case of upside-down operation of the guides, the obtained safety factor is higher than the requested one.

5.6.1 Rails adapters

Some components are modeled to fix the rails on the main plate; they are shown in Fig. 5.26 and 5.25. They consist of an S355JR block, on which the threaded holes for the rail connection have to be machined; the simple adapter measures $820x38x16$, while the other is bigger measuring $820x38x18$. In this way, it is possible to machine a recess for the positioning of the rail, with a depth of two millimeters. These adapters have to be welded to the main plate; for both the elements the holes are for screws M8x12. Fig.5.27 shows a section of the component.
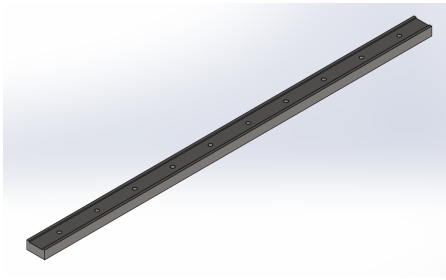
Figure 5.25: Rail adapter with referencing elements
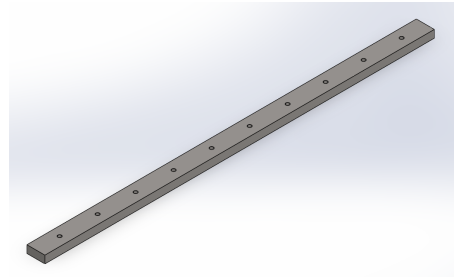
Figure 5.26: Rail adapter
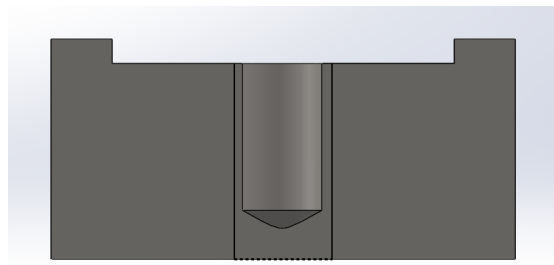
Figure 5.27: Section of the adapter showing hole and recess

5.6.2 Welding computation

To dimension the welding between the main plate and the rail adapters, the Eurocode 3 procedure is used: this procedure is suitable for the steel S235, S275, S355, S420, and S460, static verification, when using butt welds and fillet welds. In this case, it is chosen to use a fillet weld to be realized along the length of the components on both sides. Figure 5.28 shows the considered stresses inside a welding:

- σ is the compression or tension normal to the beam axis;

- τ is the tangential tension along the beam axis

- l is the length of the welding

As resistant section, it is considered:

$$A_{res} = L * a \tag{5.13}$$

where L is the length of the welding and a is the welding height, corresponding to the height of the triangle inside the beam, p is the cathetus of that triangle. Using
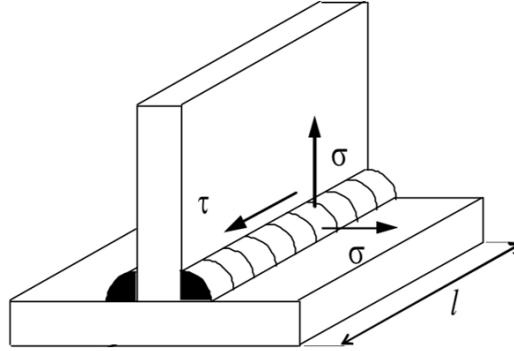
Figure 5.28: Stressed in the weld

the Directional Method, there are several tensions in the weld throat (see Fig.5.32). To verify the weld, the following inequalities have to be fulfilled:

$$\sqrt{\sigma_\perp^{g2} + 3 * (\tau_\perp^{g2} + \tau_\parallel^{g2})} \leq f_u/(\beta_W * \gamma_{M2}) \tag{5.14}$$

and

$$\sigma_\perp{}^{g2} \leq 0.9 * f_u/\gamma_{M2} \tag{5.15}$$

where:

- $f_u = 510 MPa$ is the breaking load of the base material;

- $\gamma_{M2} = 1.25$ is the safety factor;

- $\beta_W = 0.9$ is the correlation factor.

To verify the welding, it is assumed to have a load of $P = 1000N$ that pulls the adapter from the plate, as shown in Fig. 5.30. This value is obtained considering all the masses attached to the main plate through the welding: they consist in two suction cup rows, two rails, four slides, the heaviest box, and the two adapters. It is considered an acceleration of three g, giving $P = 883N$, which is increased to the shown value. The welding offers a reacting force F, which has to be decomposed in parallel and perpendicular components, as shown in Fig. 5.31. After the forces are computed, it is possible to find the tension and check the inequalities, using a throat height $a = 5mm$ for the computations.

$$A_{res} = a * L = 5 * 820 = 4100 mm^2 \tag{5.16}$$

$$F = P/2 = 500N \tag{5.17}$$

$$F_{//}^g = F_\perp^g = F * \sin 45 = 353{,}5N \tag{5.18}$$

$$\sigma_\perp^g = F_\perp^g / A_{res} = 0.086 MPa \tag{5.19}$$

$$\tau_\perp^g = F_{//}^g / A_{res} = 0.086 MPa \tag{5.20}$$

In addition, it is verified that:

$$\sqrt{0.086^2 + 3 * 0.086^2} \le 510/(0.9 * 1.25) = 0.172 \le 453 \tag{5.21}$$

and:

$$0.086 \le 0.9 * f_u / \gamma_{M2} = 0.086 \le 367.2 \tag{5.22}$$

So the chosen welding can be used. To perform the welding it is necessary to place the adapters with a $10mm$ gap from the extremities of the plate; Fig. 5.29 shows the 3D model of the assembled components including a rail, an adapter, and the cosmetic weld.
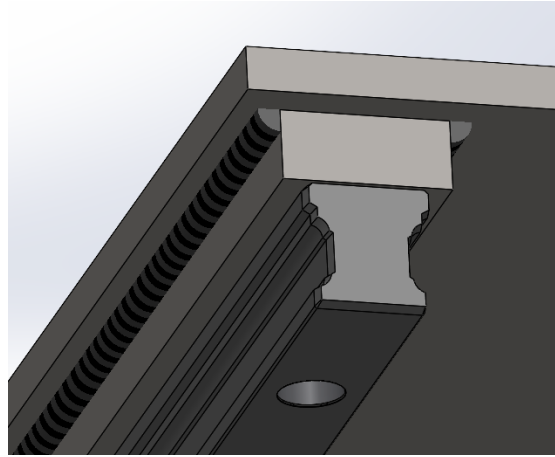
Figure 5.29: Assembly of the rain with the adapter and welding on the plate

5.7 Robot flange adapter

In order to assemble the gripper on the robot flange, a custom piece is designed. The component is made of a steel S355JR plate, and works as an interface between the gripper main plate and the robot flange; a view of the component is presented in Fig. 5.33. It measures $250x250mm$ and has a thickness of $18mm$. The component has different holes for mounting with the other parts: in the inner part there is a pattern of six circularly distributed passing holes, in the bottom part of the plate these holes have the cut for the screws' heads. The used screws are M10 with cylindric head. The positioning on the flange is guaranteed by $\phi 10mm$ holes for a positioning pin, as present on the robot side. The outer eight passing holes are
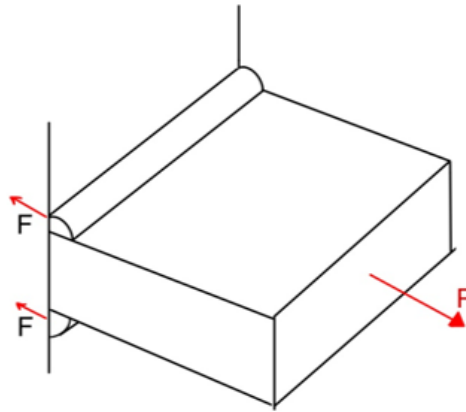
Figure 5.30: Applied load
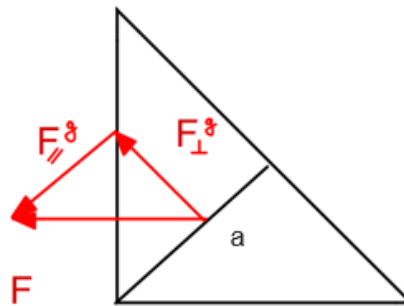
Figure 5.31: Reacting forces on the throat section

meant for the assembly of the adapter to the main gripper plate. This is done by the top of the component using M10x25 screws, that screw into the main plate threaded holes. The used class of screws should be at least 8.8; Fig. 5.34 shows the considered load condition: to the lower plate is applied a vertical force given by all the masses attached to the main plate $m \approx 59kg$ with an acceleration of $3g$, enlarged by 20%.

$$F = m * 3 * g * 1.2 = 2075N \qquad (5.23)$$

Each screw has a load of $C/8 \approx 260N$. To verify the connection, the following inequality must hold:

$$X * R_{p02} + \Delta\sigma_{max,v} \leq R_{p02} \qquad (5.24)$$
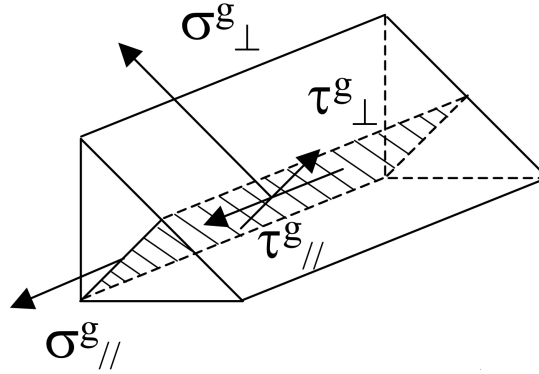
Figure 5.32: Stress in the throat section
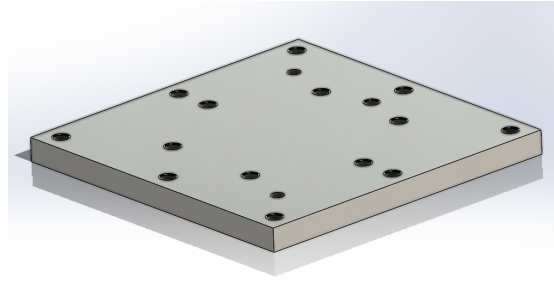
Figure 5.33: Robot flange adapter

where X is the fraction of the elastic material limit at which the screw is mounted, typically $X = 0.9$, $\Delta\sigma_{max,v}$ is the tension of the screw given by the load partition between the screw and the fixed pieces, and R_{p02} is the yield strength of the screw material. It is necessary to estimate the deformability of the screw and the fixed pieces as follows:

$$\delta_p = \frac{L_p}{E_p * A_p} = 5.57 * 10^{-7} \tag{5.25}$$

where $E_p = 210000 MPa$ is the modulus of elasticity of the material, $L_p = 18mm$ is the height of the piece, and A_p is computed as follows:

$$A_p = \frac{\pi}{4} * ((d_k + 0.1 * L_p)^2 - d_h^2) = 153.81 mm^2 \tag{5.26}$$

where $d_k = 16mm$ is the head screw diameter, $d_h = 11mm$ is the diameter of the through hole. The screw deformability is computed as follows:

$$\delta_v = \frac{l}{E_v * A_v} = 1.86 * 10^{-6} \tag{5.27}$$

where $l = 25mm$ is the screw length, E_v is the screw material elastic modulus, and A_v is the resistant section of the screw, computed using the mean diameter:

$$A_v = \frac{\pi * d_m^2}{4} = 63.98mm^2 \qquad (5.28)$$

The portion of the load acting on the screw is:

$$\Delta C_v = C * \frac{\delta_p}{\delta_v + \delta_p} = 59.9N \qquad (5.29)$$

The corresponding tension in the screw is computed using the minor diameter d_n of the screw:

$$\sigma_{max,v} = \frac{\Delta C_v * 4}{\pi * d_n^2} = 1.14MPa \qquad (5.30)$$

Substituting in (5.24), it results:

$$X * R_{p02} + \Delta\sigma_{max,v} \leq R_{p02} = 0.9 * 640 + 1.145 \leq 640 = 577{,}14 \leq 640 \qquad (5.31)$$

It is checked that the friction force generated between the surfaces is higher than a possible shear force between the plate and the adapter in the case of a lateral acceleration; the minimum force that the screw should apply is then computed as:

$$F_p = \frac{F * CS}{f * n * m} = \frac{2075 * 1.25}{0.3 * 8 * 1} = 1080.73N \qquad (5.32)$$

where F is the total load, CS is a safety factor, f is the friction coefficient, n is the number of screws, and m is the number of surfaces between the pieces. Mounting the screw at $X * R_{p02}$ gives a force on the screw of:

$$F_v = X * R_{p02} * A_r es = 30124.8N \qquad (5.33)$$

which is higher than F_p.

5.8 Extruded profiles movement

As previously explained, the slides of the electric axis have the only function of dragging the extruded profile. It is necessary to model a coupling between them that can provide this feature without realizing a permanent fixture in order to not have any blocking in case of misalignment of the components. Among all the possible solutions, it is chosen to adopt a system composed of two elements: a block that is fixed to the grove of the extruded profile, and an L-shaped fork piece that is mounted on the axis slide and can grab onto the first block. Fig. 5.35 shows the latter element; the biggest side of the element is to be mounted on the slide of
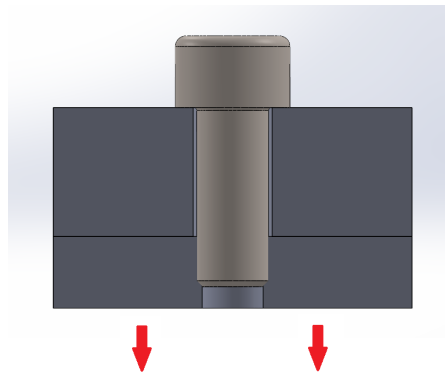
Figure 5.34: Screw load

the electric axis in its center. This connection is done using four M5x10 screws that pass in the four holes and screw into NST-5-M5 nuts, which are placed inside the grooves of the slides. The cutout in the lower side is the housing for the block, which is shown in Fig. 5.36; the protrusion in the lower end of the component goes into the grove of the extruded profile, and the whole block is fixed on it using an M8x16 cylindric head screw. In this way the screw is not subjected to shear stress but provides only the positioning for the block, which pushes directly against the walls of the groove. The L-shaped component is subjected to a FEA analysis
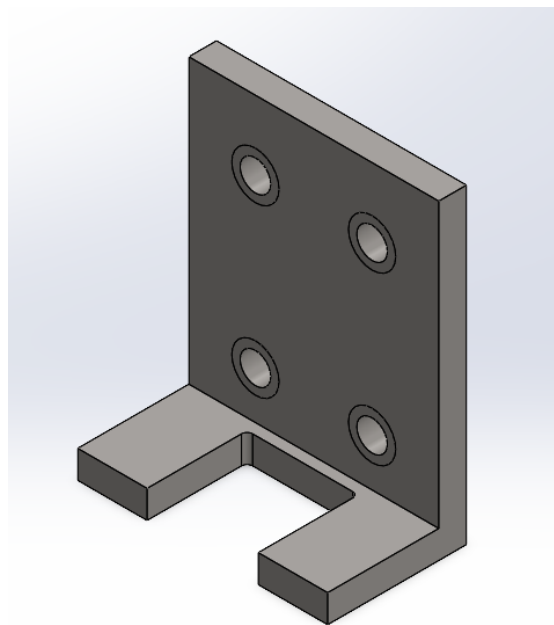
Figure 5.35: L-shaped fork piece

60
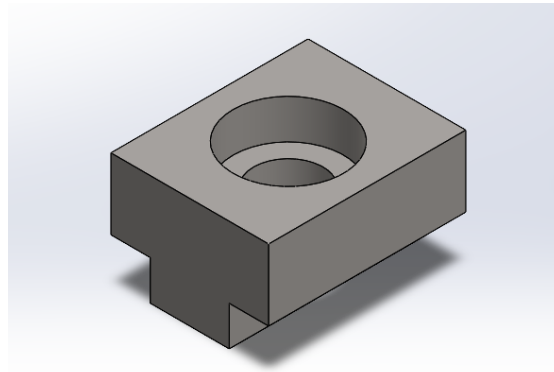
Figure 5.36: Block for the movement

to see its behavior in a hypothetical load condition. The imposed conditions are similar to the ones seen in the suction cup unit mount. Fig. 5.37 shows the mesh used for the analysis; it is a high-quality mesh. As before the figure shows the distribution of the jacobian ratio; in this case, the minimum value is 1 and the maximum is 2.897. The mesh details show that there are no distorted elements and 99.9% of the elements has a aspect ratio lower than three, showing an overall good quality. Regarding the applied constraints, the presence of the screw connection is given by locking the radial movement of the holes, fixing the section of the surface corresponding to the screw heads, and the presence of the axis slide is simulated with a virtual wall placed behind the piece. Regarding the load it is assumed to have a $400N$ load applied on one of the inner faces of the cutout, as the block was pushing on it, the load accounts for the masses of the suction cup rows, the two slides of the linear guide, and the heaviest box, equal to $10.2kg$, subject to an acceleration of $3g$, the value is then enlarged by thirty percent. The results in terms of von Mises tension and deformation are shown in Fig.5.13 and 5.14, denoting a low maximum tension in the piece and very small deformations. Finally, it is reported a view of the configuration of the axis slide and the suction cup row using the explained solution in Fig. 5.40.

5.9 Optoelectronic sensor mounting brackets

The gripper is intended to have a pair of sensors to check if the box to be grasped is effectively present under the suction cups. The sensor has to be unified to the extruded profile to always check under the cups. A simple bracket is modeled, composed by a small plate that can be bent into the desired shape. The component is provided with a hole for the screw to connect to the profile and a hole for a pin to lock its rotation around the screw. The last machinings in the component are to position and adjust the angle of the sensor; the mounting has a thickness of $4mm$
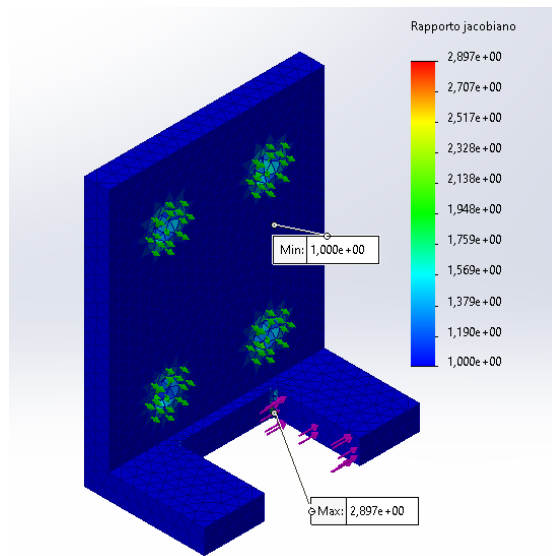
Figure 5.37: Utilized mesh for the analysis, constraints and load
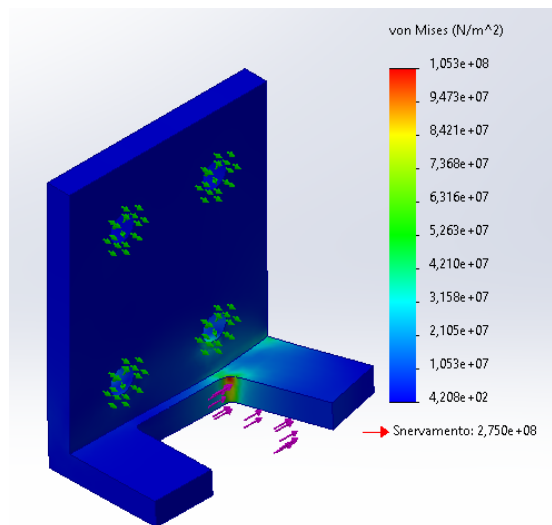
Figure 5.38: FEA results for stresses

and is realized of S355JR steel. The bending of the plate is set to 30°; a real-world test can determine if this value is suitable, moreover the component could be made by lighter material and thinner. The bracket is shown in Fig.5.41; it has to be fixed to the bottom side of the extruded profile, so opposite to the electric axis slide.
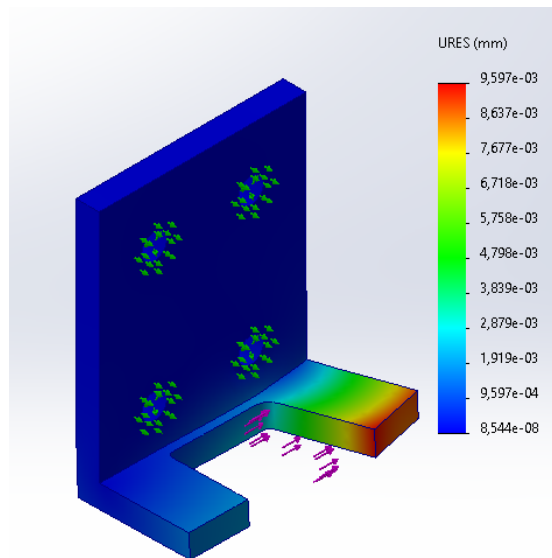
Figure 5.39: FEA results for displacement
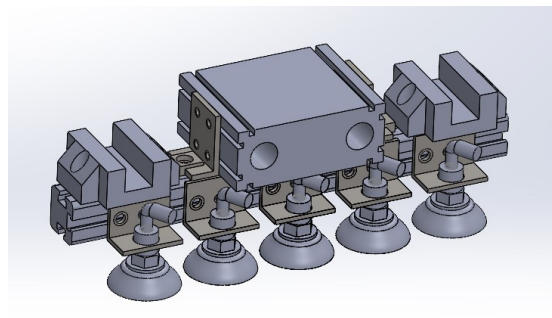
Figure 5.40: Axis slide and suction cup row assembly

5.10 Gripper mock-up and connections

Figures 5.43 and 5.42 show the final mock-up of the gripper; all the components are now enumerated according to the pictures:

1. Festo stepper motor

2. Festo gear reduction

3. Festo mounting kit

4. Custom main plate

5. Custom robot flange adapter

Figure 5.41: Provisional bracket for piece detecting sensor

6. Mounting bracket for pressure sensor

7. Mounting holes for Festo VN-07 vacuum generator

8. Festo SPAN-B pressure sensor

9. Festo MUE-45 mounting element

10. BOSCH rexroth FKS 1665 slide

11. Custom suction pad unit L-shaped mount

12. Custom rail adapter

13. BOSCH rexroth rail

14. Festo ELGG-TB-200-H electric axis

15. BOSCH rexrot extruded profile 40x40-3N

16. Festo SOOE distance sensor on the custom mounting bracket

17. Suction cup unit

The tubes used for the vacuum circuit are not represented in the mock-up along with the distribution elements; their positioning has to be determined according to the tube flexibility in a real-world assembly. The following list contains the used connecting elements used in the mock-up and their functions:

- The rail adapters are fixed to the main plate by a fillet weld.

- The rails are mounted on the rail adapters using ten M8x25 screws each.

- The linear guide slides are fixed to the extruded profile using two M8x20 screws and two hammerhead N10 nuts.

- The suction cup units are fixed to the L mount, which is fixed on the extruded profile using one M8x12 and one N10 nut, along with one or two centering pins.

- The MUE-45 mountings are fixed to the main plate using two M5x10 screws, and eventually a centering pin

- The robot flange adapter is fixed to the main plate through eight M10x25 screws, and two centering pins.

- The sensors' brackets and the vacuum generators' brackets are fixed to the main plate using M6x12 screws.

- The distance sensor is mounted using M8x16 screws
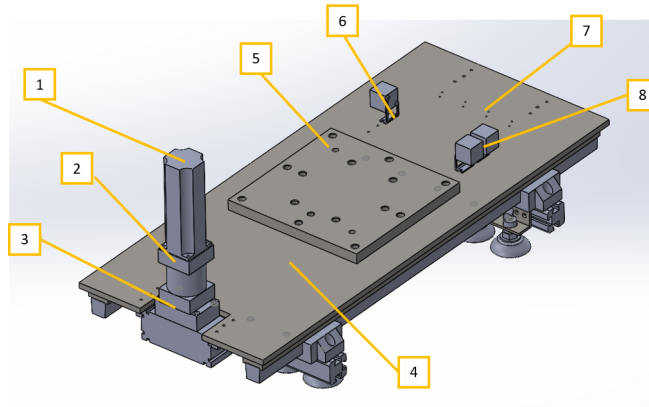
Figure 5.42: Top view of the gripper mock-up

5.11   Main plate and flange adapter static analysis

A static analysis is performed on the main plate to check, under some assumption, if it can withstand the loads applied to it during the movement. The analysis is performed on the assembly composed by the main plate and the adapters for the linear guides rails. The following assumptions are made:

- the plate and the adapters are simulated as one body; they are bonded together, in this way the load is guaranteed to be transferred between the components;

- the rails are inserted in the simulation as distributed masses on the adapters;
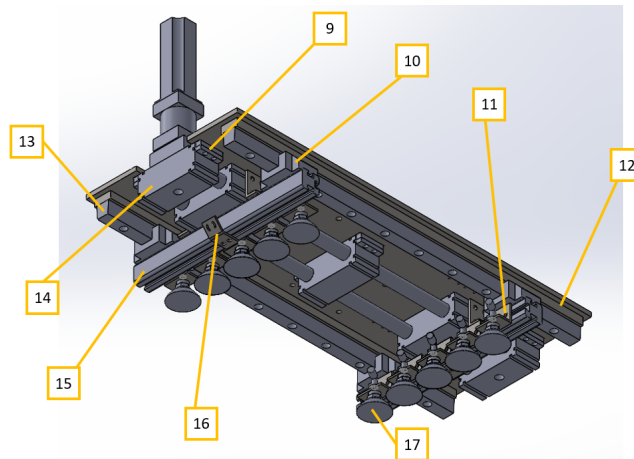
Figure 5.43: Bottom view of the gripper mock-up

- all the components attached to the gripper are considered rectangular solids, with uniform mass distribution;

- the rigidity of the axes and the rails are not taken into account.

Given the assumptions made, the results will give only an approximate view of the plate behavior. The main scope of the analysis is to check the bending of the plate and the tensions in the material. To perform the analysis, an assembly with the parts of interest is first created (Fig. 5.44), then it is converted into a high-quality mesh.
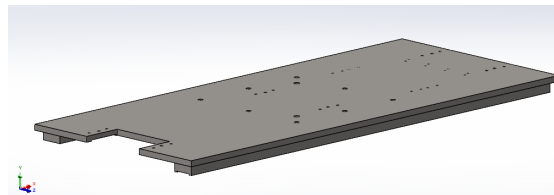
Figure 5.44: Assembly used for the analysis

To evaluate the quality of the mesh, the aspect ratio and jacobian ratio graphs are produced; they are reported in Fig. 5.45 Fig. 5.46. The aspect ratio has a minimum value of 1.052 and a maximum of 15.63, the jacobian ratio of the elements is between 1 and 28.43. The details of the mesh provided by the software show that there are no distorted element, and the 94.1% of the element has an aspect ratio lower than three, only 0.1% of the element have an aspect ratio higher than ten. After the evaluation of the mesh, the constraint and loads are applied: a fixed constraint is applied to the inner surfaces of the holes for the coupling with
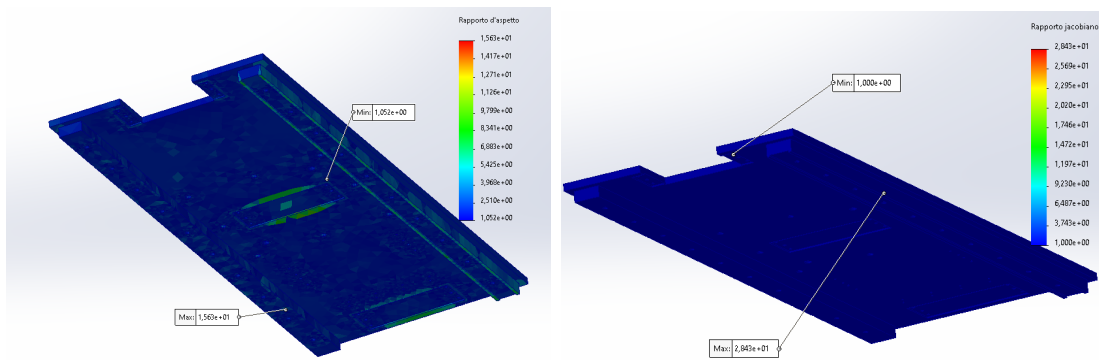
Figure 5.45: Mesh aspect ratio graph **Figure 5.46:** Mesh jacobian ratio graph

the robot flange adapter; the components mounted on the gripper are considered rectangular solids with the same mass and uniform density; they are added to the simulation as remote masses, provided with the inertia value. The remote masses are located in the center of mass of the corresponding simple solid. The masses are connected to the surfaces where the actual components act using simulated rigid bars, the connection type is set to distributed to not stiffen the surface. The remote masses relative to the axis, the mounting kit, the gear, and the motor, are connected to the lower portions of the plate, where the blocks of the electric axis are placed; while the ones for the suction cup rows and the box are connected to the lower surface of the rail adapters, where the rail are mounted. The rails are added as distributed masses placed on the same surface. Fig. 5.47 shows the placement of all the loads; for the boxes it is used the mass and dimensions of the heaviest one, corresponding to line F. The suction cup rows are placed in the furthest positions possible on the axis; the red arrow indicates the acceleration of $3g$ applied. The analysis is performed several times, changing the direction of the
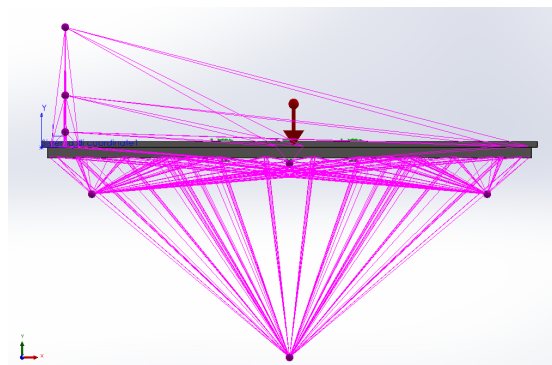
Figure 5.47: Loads placement for plate static analysis

applied acceleration. The main scope of the analysis is to check the displacement of the plate, since the electric axis can malfunction if it has a deflection of half a millimeter. Fig. 5.48 shows a comparison of the results in terms of resulting
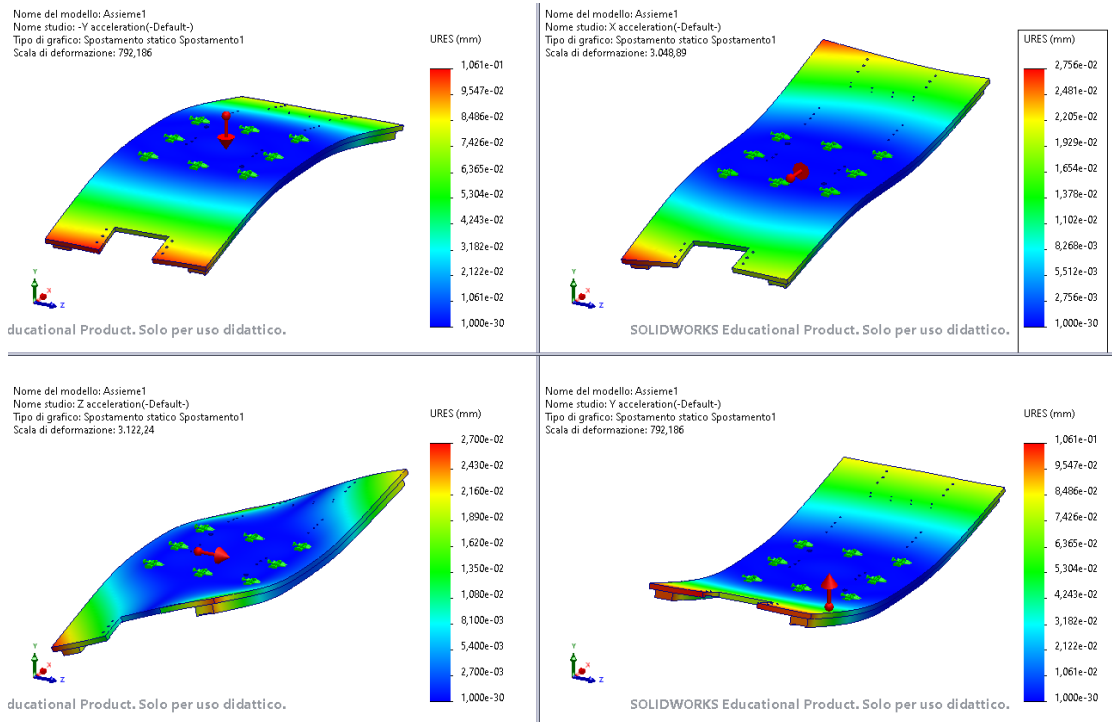
Figure 5.48: Comparison between resulting displacements changing the acceleration direction.

displacement. The maximum displacement occurs with the acceleration directed as $-y$, reaching $0.1061mm$; regarding the von Mises stress, the maximum value is $39.82MPa$ corresponding to the edge of the mounting hole shown in Fig. 5.49. The plastic limit of the material iron S355JR $275MPa$ is not reached; moreover, the high-stress points, which are located around the mounting holes, are far from the mesh section with a high aspect ratio or jacobian ratio. The flange adapter is then subject to a static analysis; the model is converted into a mesh, which has no distorted elements and 98% of the elements have an aspect ratio lower than three. Fig. 5.50 shows the applied load: the rest of the gripper is simulated as a rectangular solid with dimensions $l_x = 400$,$l_y = 145$,$l_z = 840mm$, according to the reference frame of Fig. 5.50 and a mass $m = 58.756kg$ with uniform density, and expressed as a remote mass, positioned in the center of mass of the solid and centered to the flange adapter, connected to the main plate mounting holes surfaces. The analysis is performed three times with an acceleration of $3g$ along the main directions. To replicate the connection to the robot flange, a virtual

68
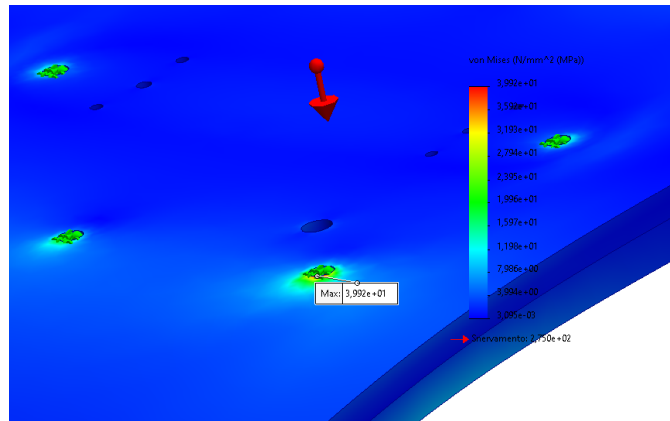
Figure 5.49: Maximum von Mises stress

wall interaction is applied on the circular section of the model shown in Fig.5.50. The radial translation of the mounting holes and the normal translation of the surfaces under the screw heads are fixed using the advanced constraints shown in Figure 5.51. The resulting von Mises stresses and displacements of the plate are
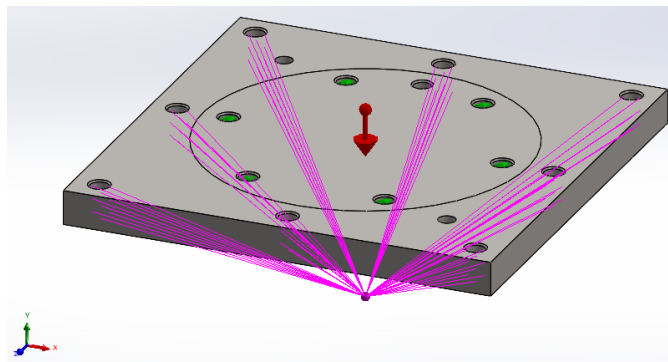
Figure 5.50: Flange adapter model applied load

compared in Figures 5.52 and 5.53; the plastic limit of the material is not reached and the displacement values are very low.
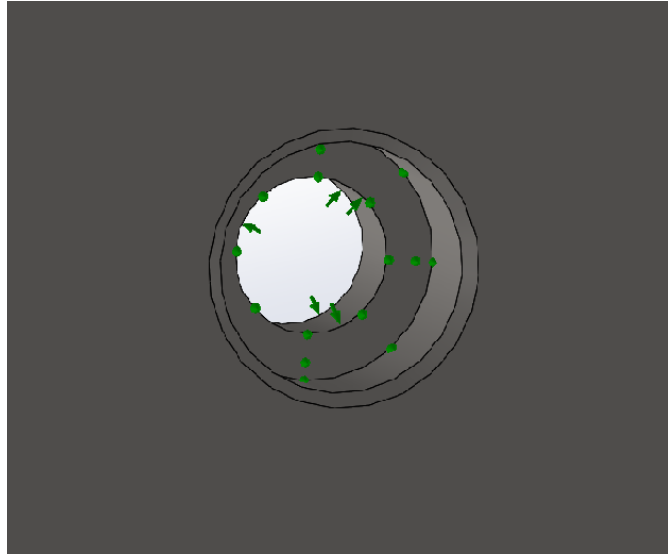
Figure 5.51: Applied constraints
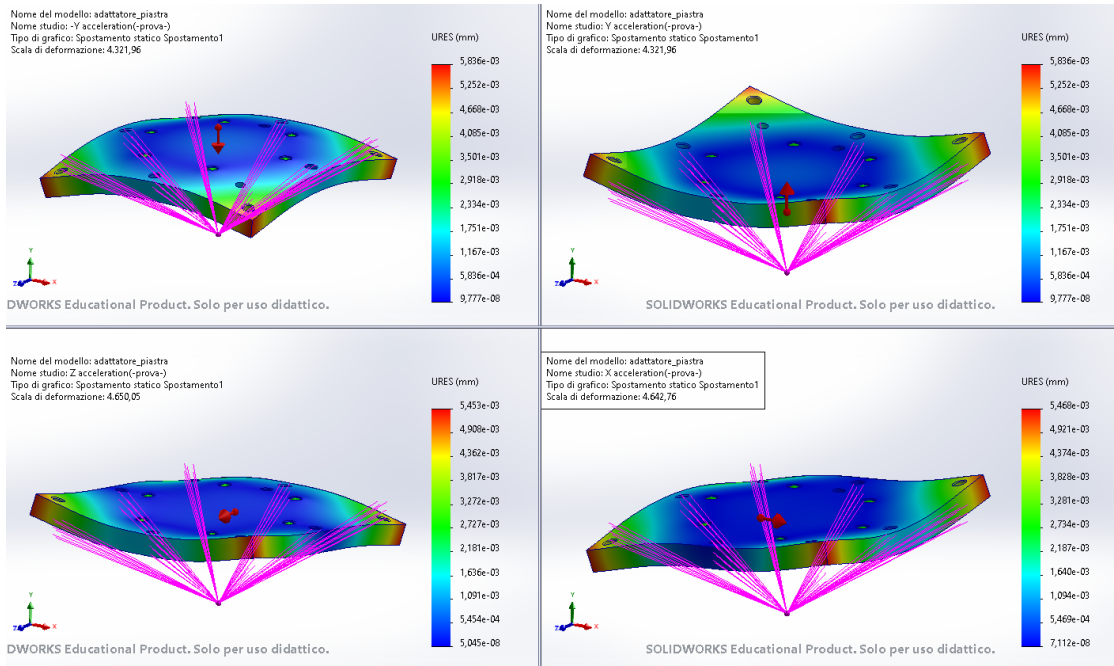
Figure 5.52: Displacements comparison
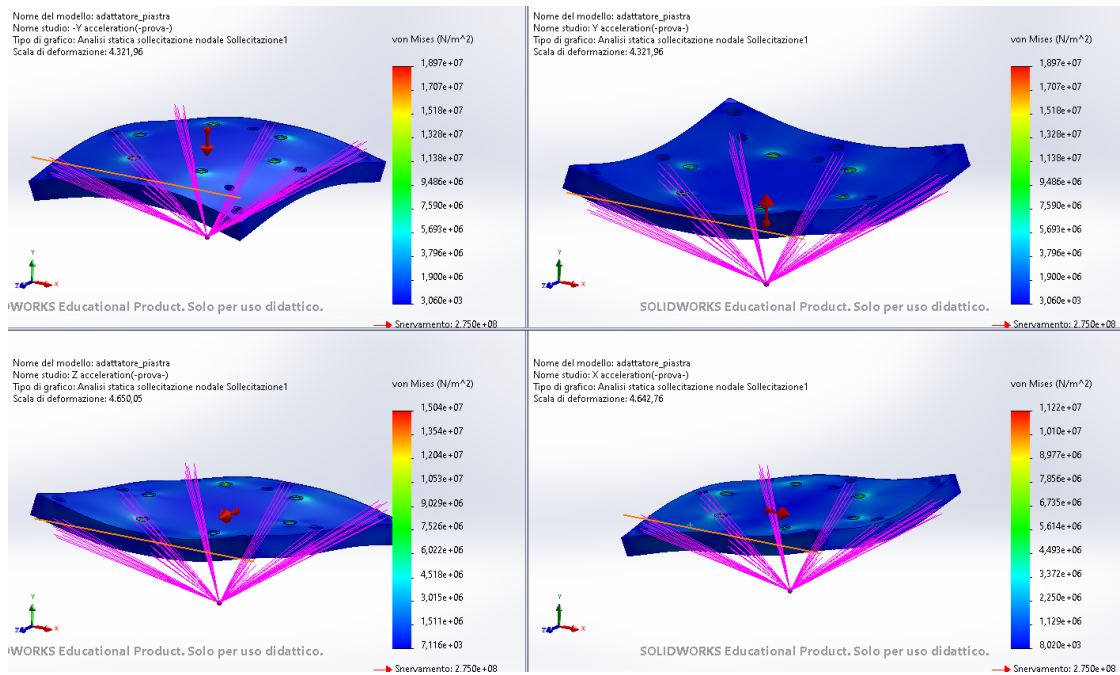
Figure 5.53: von Mises stresses comparison

Chapter 6

Electric design and control

The main feature of the designed gripper is its flexibility, so its capability to change its working dimensions according to the object to be grasped. The previous chapters explained how the mechanical and pneumatic designs are done with this feature as an objective, the same has to be done for the electronic and software sides of the device. In this chapter, all the selected electrical components are shown and described. The goal is to provide a high-level diagram showing all the connections between components; finally a control strategy is shown, with a particular focus on the function to be implemented in the robot controller to work with the designed gripper.

6.1 Functionalities and components selection

All the components shown in the previous chapters have some kind of electric or electronic interface, to function as desired. In a hypothetical scenario, the gripper is intended to be managed directly by the robot controller, without the need for any extra device such as a PLC, which is a programmable logic controller, or an industrial device used to automatize processes such as an assembly line. This is done to keep a simple solution that can directly communicate with the robot, leaving the robot itself to be a slave of a higher-order PLC controlling the whole process. The following list shows all the expected functionalities of the gripper:

- the device must be able to adapt itself to the box dimension, whose value is available in the robot controller;

- the device must be able to perform a homing routine for the electric axis in order to obtain a precise positioning of the suction cups;

- the device must be able to activate independently each of the vacuum zones;

- the device must sense if each vacuum zone is working properly, or if the target pressure is not reached;

- the device must know if there is an object to be grasped under the suction cups;

- the device must be capable of communicating the previous information to the robot controller in a reliable way.

To obtain these features it is chosen to exploit a communication based on boolean values exchanged between the robot controller and the gripper through digital inputs and outputs.

6.1.1 Electronic components for vacuum circuit

In Chapter 4, it is explained that the vacuum generator and a pressure sensor are needed in the pneumatic circuit. The SPAN sensor, in particular, has an operating voltage between $10.8V$ and $30V$, it is selected for its working principle: the sensor has a PNP or NPN output that can be configured also to be normally closed or normally open, as seen in the schematic view in Fig.6.1. The sensor offers different switching functions, depending on its settings. The first working mode consists of a threshold comparison: two pressure teach points, $TP1$ and $TP2$, have to be set in the device, which uses $SP = TP1 + TP2/2$ as threshold value; when the read pressure reaches SP coming from $TP1$ the output will switch and vice-versa. The second mode is a window comparator: two teach points are provided, $TP1$ and $TP2$, the switching does not take place in the mean value, but at $SP.Lo$ and $SP.Hi$ corresponding respectively to $TP1$ and $TP2$, this results in the output being either high or low, depending on the N/O or N/C configuration, when the read pressure is between the specified values, the different modalities are shown in Figures 6.3 and 6.2
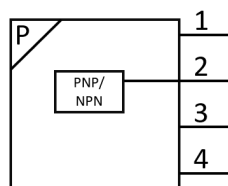
Figure 6.1: SPAN-B schematic representation

For the particular application, it is chosen to use the threshold comparator function, because the calculation about the necessary pressure done in Chapter

4 established a minimum vacuum level to be reached, so the sensor has only to communicate to the robot if this happens. Regarding the normally open or normally closed output, it is chosen to use a normally open configuration, so a high signal will indicate the reaching of necessary conditions. The sensor has two push buttons and a display that are used to set all the parameters and show the read values. The switching points are set using teach-in, so creating the required pressure in the sensor and storing it in the device using the corresponding key combination. Fig. 6.1 shows a schematic view of the sensor; the electrical interface is composed of four connections:

- *pin*1 is the input for $24VDC$;

- *pin*2 is the switching output;

- *pin*3 is not connected;

- *pin*4 is the input for $0VDC$;

The sensor needs a connecting cable Festo NEBS-L1-G4-K-5-LE4 that provides the required four internal connections and has an open end.
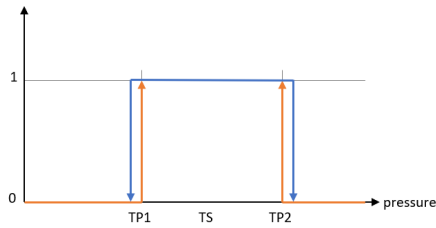
Figure 6.2: output vs. pressure reading for window comparison mode and normally open contact
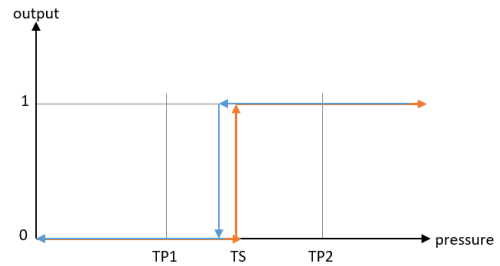
Figure 6.3: Output vs. pressure reading for threshold comparison mode and normally open contact

The selected vacuum generator Festo VN-07-H-T3-PQ2-VQ2-RO1-M is equipped with an electric valve that activates the vacuum generation; the latter is the only additional function of the generator, it has no other sensors to monitor its functioning since this function is done by the SPAN device. The vacuum generator has an interface for plugging in a connector model NEBV-H1G2-KN-1-N-LE2 provided with two internal connections and open end; so, to trigger the vacuum generation it is only necessary to apply a tension between $21.6VDC$ and $26.4VDC$, through this connector. The manufacturer indicates a power of $1.2W$ for the generator so a current absorption, working at $24VDC$ of:

$$I = W/V = 1.2/24 = 0.05A = 50mA \tag{6.1}$$

74

6.1.2   Box presence sensors

In a working condition, after the robot puts the gripper over the box to be grasped, it is necessary to check if the object is present before contacting it and activating the vacuum. There are several types of sensors available on the market, using different principles to sense the object. Electro-mechanical sensors detect physical contact with the object outputting a signal; these are suitable when the objects can be touched. Magnetic sensors instead, can detect the presence of a magnetic object narrowing their application to magnetic material. Inductive sensors can detect the changing of the electromagnetic field created by the sensor itself, working with objects made of metal. capacitive sensors can detect an object monitoring its dielectric constant. Finally, photoelectric sensors use a beam of light emitted by a laser or a diode to sense an object; there are different technologies for this kind of sensors, the most common ones have an emitter and a receiver; the object is detected when the latter can not receive the emitted light. In other cases, the emitter and receiver are in the same device and a reflector has to be placed in front of it; also in this case when the object blocks the reflected beam the sensor triggers. Finally, there are sensors that use the light reflected by the object itself to sense it, they are known as diffuse sensors. Having to work with cardboard boxes that can be assumed to have a similar surface finish and similar color, it is decided to use a photoelectronic sensor. The particular model is the Festo SOOD-BS-R-PN-80, which is a diffuse sensor with background suppression, it is mounted with the bracket shown in Fig. 5.41 to face under the central suction cup of the row. This sensor has a maximum sensing distance of $80mm$, works with a tension of $24VDC$ and has a PNP or NPN output. A schematic view of the component is reported in Fig. 6.4, where pins 1 and 2 are respectively the input for $24VDC$ and $0VDC$, pin 4 is the output, the connection is realized through a three pins interface on the sensor with a M8x1 plug. The output of the sensor will be high if an object is
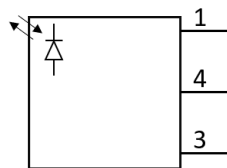
Figure 6.4: SOOD sensor schematic

placed at a sensing distance.

75

6.2   Motor controller

The main feature of the gripper is the possibility of changing the suction cups position. The mechanical components necessary for this goal are reported in Chapter 5. The electric axis used for the movement needs a control unit, which has to be coupled to the motor to position it and perform other tasks, such as homing. The selected motor family is the EMMS-ST, corresponding to stepper motors, [7] the working principle of a stepper motor is described in [7]: first of all, such motors can be divided into two main categories, which are permanent-magnet and variable-reluctance. For both of them, the main principle is similar. The first category is characterized by a magnetized rotor with one or several pairs of poles diametrally placed, the stator is placed outside the rotor. It has several windings that can be excited to produce a magnetic field; when this is done, the rotor tends to align to the produced field determining the rotation of the shaft. The movement of the motor is determined by the energizing sequence of the windings. With four windings, it is possible to obtain three different modes, each one with different power absorption or step angle, which is the angle described by the rotor when one impulse is provided. In the variable-reluctance category, there are several rotors fixed to the shaft, one for each phase, and a corresponding number of independent stators. When one of the phases is energized, the corresponding rotor aligns itself to it. The key for the component is to have the three rotor phases placed on the shaft with a small angular offset, in this way when the stators are exited in sequence, the shaft follows them in a rotational movement. A stepper motor needs a controller to provide the required signal to its coils; moreover, such a device can perform by itself position, velocity or torque controlled motion. The motor manufacturer proposes several devices to be coupled to a stepper motor, and many of the solutions require the presence of a PLC that runs particular libraries to manage the movement of the motor. For the gripper under study it is chosen to utilize a motor controller that can be managed using only digital inputs and outputs that are provided directly by the robot controller. The selected motor controller is the CMMO-ST-C5-1-DIOP; the device communicates with the robot controller via its X1 I/O interface that has a PNP switching logic.

6.2.1   Motor controller interfaces

As reported in Fig. 6.5, the device has several interfaces for its integration in an automation application; they correspond to:

1. Power supply port

2. I/O PNP logic port

3. Ethernet port

76
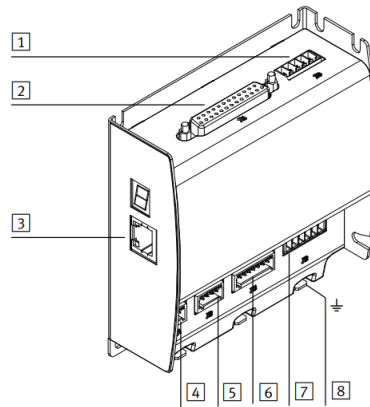
Figure 6.5: Festo CMMO-ST interfaces, from Festo manual

4. Reference switch port

5. STO port

6. Encoder port

7. Motor port

8. Earth connection

The device is also equipped with a small display that shows its current operation. The X1 I/O port offers twenty-five pins: the first eleven are for digital inputs, the next ten are for the digital outputs, pin twenty-four is a $+24V\,DC$ logic output and pin twenty-five is the $0V$ connection, pin twenty-three is not used. Control signals are exchanged through this interface; a $24V$ tension corresponds to an high signal, while a $0V$ tension corresponds to a low signal. The X1A port is used to connect the reference switch of the axis; this is mandatory when doing a homing operation: once the slide reaches the end of the axis, the switch provides a signal to the motor controller that can store that position as the home point of the axis. The used sensor is the Festo SIES-8M-PS-24V-Kx-OE, where x indicates the cable length. The sensor is mounted on the ELGG axis through a bracket fixed to the groove of the block; on the moving slide of the axis a metal shaft is fixed, which triggers the sensor when it moves above it. The sensor has three wires, two of them are used for the supply of $24V$ and $0V$, the other is the sensor output. The X1A port on the controller has the corresponding three pins; the motor controller can also be configured to perform homing using the block mode, in this way the end of the reference point is searched monitoring the current absorbed by the motor. When the slide of the axis reaches the end of the stroke, the torque required by the

motor starts to rise with the current, so the controller saves such position as the home point. The ports X6 and X2 are, respectively, the motor and encoder ports, they have to be connected to the motor via a specific cable. Port X3 is the STO, which means Safe Torque Off. In a test environment, this feature can be bypassed by bridging the two STO input pins to the $24V$ output pin of such interface; in a real application, the STO signals have to be provided by the robot. The port X9 is for the power connection; it has five pins, but only three are used: pin three is the input for the control electronics $+24VDC$, pin four corresponds to the $0V$ reference for load, logic, STO and I/O interfaces, pin five is the supply for the load of the device also at $+24VDC$. The port X18 provides a standard ethernet connection for the parametrization of the device using a PC.

6.2.2 Controller configuration

To configure the used controller, it is necessary to use the software Festo Configuration Tool. This software enables the user to set all the parameters for the controller in use. To do this it is also necessary to add the corresponding plugin for the CMMO-ST. A new project is created via the software interface; the first step is to add all the components for the drive unit, as shown in Fig. 6.6, where the used controller, the motor, and the axis are added. After the first step, the used control
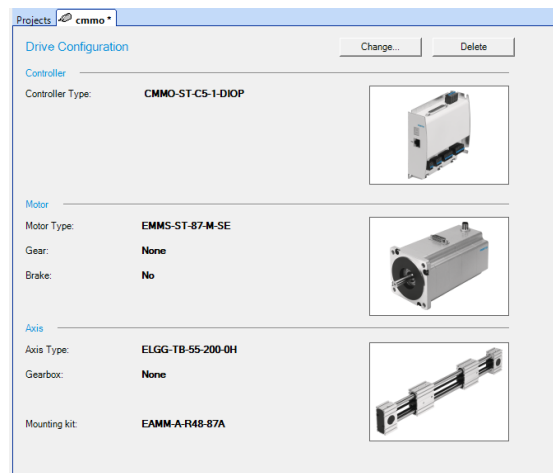
Figure 6.6: Festo Configuration Tool Drive configuration view

profile has to be chosen between the binary profile and valve profile. The first one is used, which permits to address a total of thirty-two recorded positions, while the second is limited to seven. Next a base load for the axis must be specified; a $3kg$ mass is set as the provisory value. The settings regarding the motor are left as suggested by the software. Fig. 6.7 shows the configuration for the homing of the

axis: the slide is moved in a negative direction toward the reference switch until the sensor provides a high signal. The *Parameters* panel contains the dynamic values for the reference search phase; to have precise referencing, the search velocity should be low, in this case, the default value is $8mm/s$. Performing a test on the real hardware, it is possible to find the highest search velocity that guarantees the correct homing. As an additional setting, the axis should move to the zero position after homing is complete; in this page, the homing method can be changed to 'block', in such a way the reference switch is not necessary.
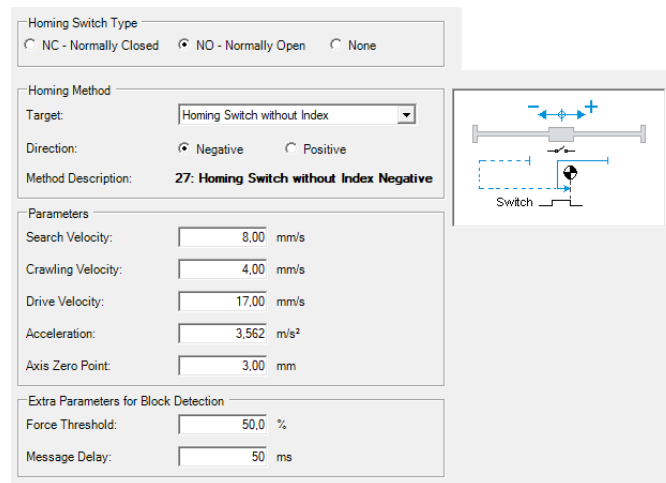
Figure 6.7: Festo Configuration Tool Homing settings

Figure 6.8 shows the working stroke for the axis, the values are added automatically by the software, based on the specified axis, and the software limits are used to limit the maximum movement of the slide, which is not sensed by any device. The software also allows the setting of two digital outputs of the controller
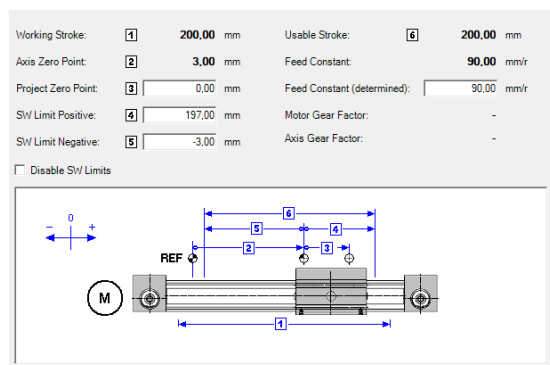
Figure 6.8: Festo Configuration Tool Axis measurements

79

to provide additional signals; in this case, they are not used. Figure 6.9 shows the basic parameter to be used for the record table. The last part of the configuration

Figure 6.9: Festo Configuration Tool Default values for record table

in Festo Configuration Tool is to define all the recordings in the record table section. Fig. 6.10 shows the interface of the record table panel in the software; each line of the table denoted by the index in the *No.* column corresponds to a different record to be stored in the device, each record can be edited as shown in Fig. 6.11.

Figure 6.10: Festo Configuration Tool Record table

The record type can be chosen between the following options:

- PA: absolute positioning value;

- PRN: position value relative to the current nominal position;

- PRA: position value relative to the current actual position;

- VSL: velocity reference value with stroke limit;

- V: velocity reference without stroke limit;

- FSL: force mode with stroke limit;

- F: force mode without stroke limit.

In this case, the first option is used, so all the positions to be recorded are expressed as absolute values from the zero point, and the value is added to the *Target* box. In *Basic Data* box, the *Start Condition* determines the behavior of the
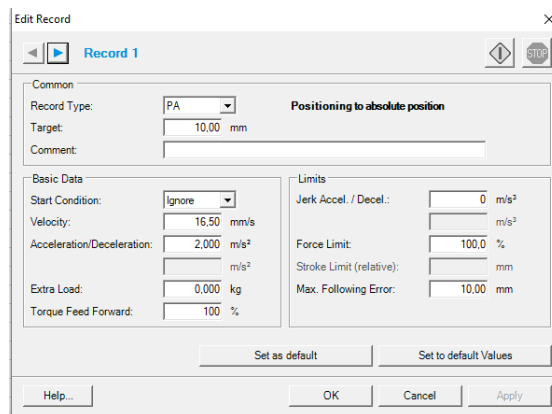
Figure 6.11: Festo Configuration Tool Edit record

controller if a new record is triggered while the current operation is still in progress. The parameter is set to *Ignore*; in this way, a new command is ignored if the current movement is not completed. Then, it is also possible to set other dynamic parameters as velocity and acceleration, which are left as default for now, and have to be tuned with hardware tests. The record table is populated with several position records that have to be defined according to the object to be grasped; each record can be triggered through five of the digital inputs of the X1 interface of the controller. This is done by expressing the index of the recording as a binary value on the five inputs; the record zero, corresponding to the low state of all the five input pins, is reserved to perform the homing.

6.3 Devices connections

Previous sections illustrated the electronic components present on the gripper. It is now shown how the various devices are connected; in this regard, a diagram is reported in Fig. 6.12, which shows the main components of the designed gripper-robot integration. On the left end of the diagram the gripper unit is represented in blue, the electronic components are shown in orange, each component is characterized by its name and eventually by the number of the same component present on the gripper. The central left block of the diagram reports the motor controller unit; in the central right end of the image the robot cabinet is reported with the I/O devices to receive and send digital signals, and in the right end the power supply is added. Orange arrows indicates the connections between the robot, the end-switch, and the motor controller, the blue arrows represent the robot output signals, the green ones indicate the robot input signals, black and red arrows represent the power supply connections. All the devices must share the same $0V$ supply.
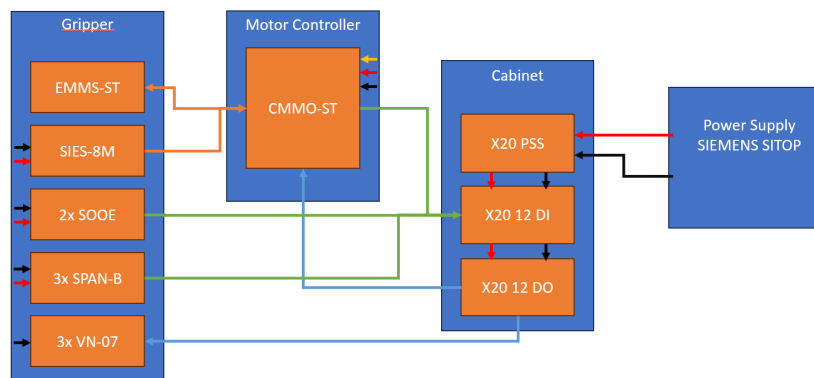
Figure 6.12: Devices connectios

6.3.1 Gripper

As previously explained, the gripper unit has several components. The motor EMMS-ST is connected to the motor controller using two cables NEMB-M12W8-E-10-LE8 and NEMB-S1W15 accounting for the drive control and the encoder signals; the end-switch SIES-8M is also connected to the motor controller. The other devices present on the gripper are directly connected to the robot; they all receive or send digital signals. Figure 6.12 also shows the power input for the devices with red and black arrows. Given the presence of two optic sensors, three vacuum sensor, and three electrically driven vacuum generators, there is a total

of five digital signals going from the gripper to the cabinet, which indicates the robot controller unit, and a total of three digital signals going from the robot to the gripper.

6.3.2   Motor controller

The motor controller requires a $0V$ connection, a $24V$ tension for the power circuit and a $24V$ tension for the logic circuit; these are provided on the X9 interface of the device. The reference switch is connected to the X1A interface, the X1 interface is used for the digital signal exchange. The pins corresponding to the signals to be used have to be connected to the corresponding I/O points of the robot controller unit; the $0V$ reference must be shared between the motor controller and the robot I/O devices. The motor controller interfaces are cabled using custom plug connectors, which are suitable for mounting in the corresponding interfaces and offer a quick connection for the cable ends and are provided with the controller. For the X1 cabling it is necessary to use a cable NEBC-S1G25-K-x-N-LE25 providing the 25 pins connector and an open end on the other side.

6.3.3   Robot cabinet

The designed gripper is intended to be mounted on a Comau NJ220 robot, which is controlled by a C5G control unit. The unit is characterized by high flexibility thanks to the modular interfaces by B&R that can be mounted in the cabinet on the internal fieldbus, which can provide auxiliary input and output. Such modular devices are intended to be used for communication with the gripper components. Many options are available for the unit, depending on the type of needed input or output. For digital interfaces, different numbers of inputs or outputs can be involved. Given the required number of inputs and outputs previously calculated, it is chosen for both input and output to use modules with twelve ports. For the digital inputs, the option is the X20-DI9371; the device is provided by the manufacturer B&R, and it is composed of three parts:

- a DI9371 digital input module;

- a terminal block for the twelve connections X20TB12 which provides push-in plugs;

- a base component X20BM11 to be mounted on the bus coupler module of the cabinet.

The option for the outputs is the X20-DO9322; it is composed of the same parts as the previous module, with the exception of the first component, which is the DO9322. The additional modules are powered by an X20-PSS Power Supply

module. It is mounted before the other modules, and provides a tension of $24V$. Once all the $0V$ potentials are connected together, the I/O interface of the motor controller and the I/O modules of the robot can be connected using single wires.

6.4   Power supply

The selected motor controller has two separate supplies for load and logic; for the load supply, $24VDC$ is required, the nominal current value for this section is $I_n = 5.7A$, while the peak value is $I_{pk} = 9.4A$; for the logic supply the required voltage is $24VDC$ with a current of $I_l = 0.3A$; the optic sensor needs a current of $I = 10mA$; the pressure sensor needs $I = 30mA$. Given the high current request of the motor controller, an additional power supply must be used, which can guarantee the peak current value to the load supply of the motor. As power supply, a Siemens SITOP PSU100M 24 V/20 A 6EP1 336-3BA10 is chosen, the device can be mounted on a normalized DIN rail, its nominal input voltage is $120 - 230VAC$ and has an output of $24VDC$, with a maximum current output of $20A$. Such a power supply is used for the supply of all the devices of the gripper.

6.5   Additional I/O modules configuration and mapping

The digital inputs, digital outputs, and power supply modules must be configured in the robot setup page and the I/O points must be mapped. The procedures are done in a virtual control unit using the software Robosim by Comau. The software IO_Cnfg is realized in Visual PDL2 and is used to add the I/O modules to the robot control unit and configure them. The software can be launched from the Setup Page on the programming terminal; after the launch in the Network tab, Powerlink must be selected to configure X20 modules. A tabular with the addable Bus Coupler devices is shown, the mounted one must be selected and added. It is now possible to add the X20 modules by pressing the X20 command: a blank tabular is shown, it is possible to add the additional modules by selecting an empty row and pressing on the Insert command. At this point the module must be selected from the visualized list and inserted. To proceed to the mapping of the I/O points, it is fundamental to add the modules in the same order as they are mounted in the cabinet. Once all the modules are added, the changes must be saved, and IO_Cnfg can be closed. Fig. 6.13 shows the IO_Cnfg page with the added modules. After the first step, it is possible to proceed with the mapping of the I/O points using the software IO_Map; as IO_Cnfg, it is available in the Setup Page of the programming terminal. After the launch, pressing the Devices command, a list of the available devices is shown; for each of them it is also
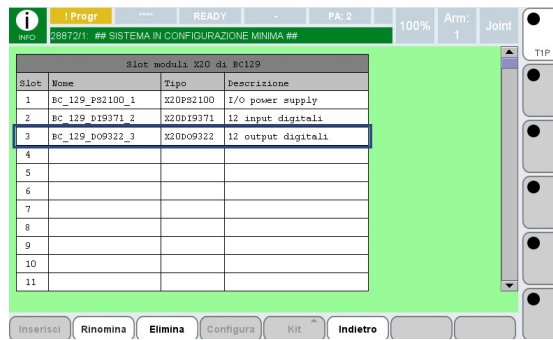
Figure 6.13: IO_Cnfg with added X20 modules

indicated the number of input bytes, the number of output bytes, and the number of already mapped I/O. After the selection of the device of interest, pressing the Modify command, a tabular with all of its inputs and outputs is displayed, each of them can be individually modified with the Modify command. Figures 6.14 and 6.15 report the pages of IO_Map showing the mapped input points. The tabulars give information about the points: Offs is the bit offset from the starting input point of the module, Pos. indicates the byte and bit corresponding to the input point, Port is the corresponding PDL2 index of the point. The Help section is used to specify the signal corresponding to the physical interface. Figs. 6.16 and 6.15 shows the mapped output points.
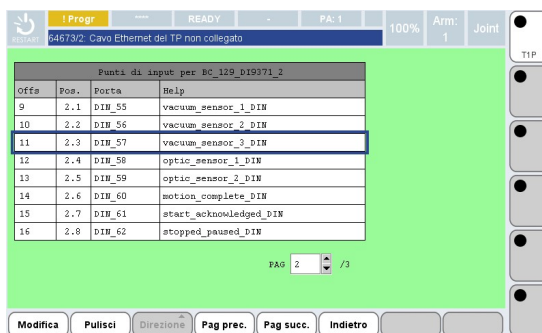
Figure 6.14: IO_Map input points for digital input module, page 1
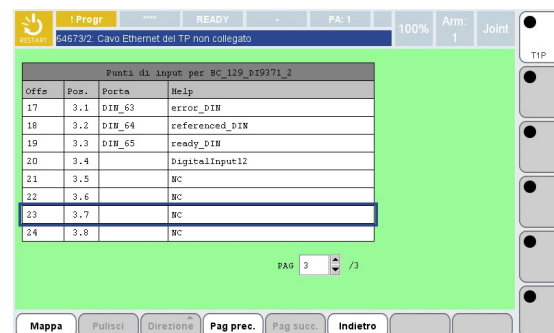
Figure 6.15: IO_Map input points for digital input module, page 2

With the mapping of all the input and output points, the modules needed to command the gripper are put into communication with the PDL2 ports for digital inputs and digital outputs, being `$DIN $DOUT`, so a PDL2 program is capable of reading or writing a digital signal if provided with the corresponding index.

Figure 6.16: IO_Map input points for digital output module, page 1

Figure 6.17: IO_Map input points for digital output module, page 2

6.6   Software implementation of the gripper

A PDL2 library containing all the functions required for the gripper control is developed. PDL2 is a programming language used to write robot programs; it is similar to Pascal and it provides elements that can be used to move the robotic arm, manage the program flow, monitor input and outputs, operate with files and implement error handling. A PDL2 program can be *Holable* or *non-Holdable*: in the first case, its execution is managed by the start and hold command, which are used in the case of motion of the robotic arm; in the other one, the execution is not managed by these commands, since a *non-Holdable* program can not contain move instruction. All the PDL2 programs have the same structure: the first line is used to identify the program with a custom name and define the additional attributes of the program, such as Holdable or non-Holdable; then, there is a declaration section where routines, constants, and variables are defined or imported, and an execution section where all the instructions are added. The following code shows the general program structure.

```
1 PROGRAM custom_name
2 CONST
3 —— constant declarations
4 VAR
5 —— variable declarations
6 BEGIN
7 —— instructions
8 END custom_name
```

A routine is a small program used for a single task; it is needed when an operation has to be repeated several times, so a program can use a routine many times calling it. When this is done, the program execution is transferred to the routine and back

to the program when the routine execution ends. Routines can be divided into procedures, composed of a set of instructions executed as a normal program and functions that return a value once the execution is done. The latter can be used, for instance, to perform math operations or check conditions, the returned type can be chosen, a routine can also use parameters. The gripper can perform a limited number of tasks, controlled by digital signal. All of them can be implemented in some routines that manage the signals and can be called when needed by the main robot program. A library containing all the routines is then developed. The library consists of a program without any instructions between the `BEGIN` and `END` statements; the program is called `GripperRoutines` and has the `NOHOLD` attribute since it does not involve robotic arm moving instructions. The declaration part contains all the mapped I/O points defined as constant values and all the routines.It is important to make all the routines available by other programs. In PDL2 a routine can be declared as public or belonging to another program; this is done with the `EXPORTED FROM` statement. To import a routine owned by another program, the statement has to be added after the routine name and followed by the name of the owner program, while to declare a routine to be public and available to other programs, the statement has to be followed by the name of the program where the routine is declared. As an alternative, the `GLOBAL` attribute can be added after the current program name; in this way other programs can use the `IMPORT` statement followed by the program whose global routines have to be imported. The realized program is reported, omitting the routines after the constant declarations which are later shown in detail.

```
1  PROGRAM  GripperRoutines NOHOLD
2
3  CONST
4      —— I/O  points
5      —— DIN
6      zone_1_sensor_din = 55
7      zone_2_sensor_din = 56
8      zone_3_sensor_din = 57
9      opt_sensor_1_din = 58
10     opt_sensor_2_din = 59
11     motion_complete_din = 60
12     start_ack_din = 61
13     paused_din = 62
14     error_din = 63
15     referenced_din = 64
16     ready_din = 65
17     —— DOUT
18     vac_gen_1_dout = 55
19     vac_gen_2_dout = 56
20     vac_gen_3_dout = 57
```

```
21      rec_bit_0_dout = 58
22      rec_bit_1_dout = 59
23      rec_bit_2_dout = 60
24      rec_bit_3_dout = 61
25      rec_bit_4_dout = 62
26      start_dout = 63
27      ctrl_enable_dout = 64
28      reset_dout = 65
29      pause_dout = 66
30
31 BEGIN
32
33 END GripperRoutines
```

6.6.1   Sensors and vacuum generators routines

Regarding the management of the sensors and the vacuum generators, four routines have been developed with different functions; the robot program should call them when some particular action are necessary. The following two routines are used to turn on or off the vacuum generation in the different vacuum circuits of the gripper. Since the generator is driven by a solenoidal valve, it is sufficient to put the corresponding digital output of the robot in a high state when the vacuum has to be activated, or in the low state when the vacuum has to be deactivated. The first line of the code reports the name of the routine; in the parenthesis, there is the parameter for the routine which is an integer and acts as the vacuum generator selector from one to three. The `EXPORTED FROM` statement with the current program name is used to make the routines available for other programs. The routines do not return any value; after the `BEGIN` keyword the instructions are added, a simple switch-case is used, depending on the provided parameter the corresponding digital output is put to high or low state. The routines end with the `END` keyword.

```
1 ROUTINE turn_on_vacuum(generator_sel : INTEGER) EXPORTED FROM
       GripperRoutines
2 ROUTINE turn_on_vacuum(generator_sel : INTEGER)
3 BEGIN
4 SELECT generator_sel OF
5 CASE(1):
6      $DOUT[vac_gen_1_dout] := TRUE
7 CASE(2):
8      $DOUT[vac_gen_2_dout] := TRUE
9 CASE(3):
10     $DOUT[vac_gen_3_dout] := TRUE
11 ENDSELECT
```

```
12  END turn_on_vacuum
```

```
1  ROUTINE turn_off_vacuum(generator_sel : INTEGER) EXPORTED FROM
        GripperRoutines
2  ROUTINE turn_off_vacuum(generator_sel : INTEGER)
3  BEGIN
4  SELECT generator_sel OF
5  CASE(1):
6      $DOUT[vac_gen_1_dout] := FALSE
7  CASE(2):
8      $DOUT[vac_gen_2_dout] := FALSE
9  CASE(3):
10      $DOUT[vac_gen_3_dout] := FALSE
11  ENDSELECT
12  END turn_off_vacuum
```

For the object presence sensors, an analogous solution is implemented. In this
case, the routine takes the index of the sensor to be checked as an argument, and
returns a boolean value to express if the object is detected or not. In the SELECT
statement, a default case is specified using ELSE; this is used by the routine when
the provided parameter is incorrect, and signals an error to the user, using the
ERR_POST function.

```
1  ROUTINE check_box_presence (opt_sensor_index : INTEGER) : BOOLEAN
        EXPORTED FROM GripperRoutines
2  ROUTINE check_box_presence (opt_sensor_index : INTEGER) : BOOLEAN
3  BEGIN
4  SELECT opt_sensor_index OF
5      CASE(1):
6          IF $DIN[opt_sensor_1_din] = TRUE THEN
7              RETURN(TRUE)
8          ELSE
9              RETURN(TRUE)
10          ENDIF
11      CASE(2):
12          IF $DIN[opt_sensor_2_din] = TRUE THEN
13              RETURN(TRUE)
14          ELSE
15              RETURN(TRUE)
16          ENDIF
17      ELSE:
18          ERR_POST(43008, ' INDEX OUT OF RANGE ',2)
19          RETURN (FALSE)
20          -- errore
21  ENDSELECT
```

89

```
22  END check_box_presence
```

Also for the vacuum sensor a similar solution is adopted; the argument of the routine corresponds to the index of the vacuum zone to check, and a boolean value is returned depending on the read pressure.

```
1   ROUTINE check_vacuum_sensor( vacuum_zone_index : INTEGER ) : BOOLEAN
        EXPORTED FROM GripperRoutines
2   ROUTINE check_vacuum_sensor( vacuum_zone_index : INTEGER ) : BOOLEAN
3   BEGIN
4   SELECT vacuum_zone_index OF
5       CASE(1):
6           IF $DIN[zone_1_sensor_din] = TRUE THEN
7               RETURN(TRUE)
8           ELSE
9               RETURN(FALSE)
10          ENDIF
11      CASE(2):
12          IF $DIN[zone_2_sensor_din] = TRUE THEN
13              RETURN(TRUE)
14          ELSE
15              RETURN(FALSE)
16          ENDIF
17      CASE(3):
18          IF $DIN[zone_3_sensor_din] = TRUE THEN
19              RETURN(TRUE)
20          ELSE
21              RETURN(FALSE)
22          ENDIF
23      ELSE:
24          ERR_POST(43008, ' INDEX OUT OF RANGE ',2)
25          RETURN (FALSE)
26      -- errore
27  ENDSELECT
28  END check_vacuum_sensor
```

6.6.2 Motor controller routines

The following routines are used to move the electric axis and manage the motor controller. The communication between the robot and the motor controller takes place through digital inputs and outputs, providing the proper signal to the motor controller. It is possible to enable it and trigger its movement, the controller gives back signals with information about its state. Table 6.1 reports all the signals that are available between the robot and the motor controller used in binary profile exchanged through the X1 interface of the latter. To make all the routines, it

is necessary to respect the timing diagram of the signals reported in the device manual, which shows which signal is the controller waiting for and what is its response.

Pin	DIN	DOUT	Description	Used
X1.1	•		Record bit 0	•
X1.2	•		Record bit 1	•
X1.3	•		Record bit 2	•
X1.4	•		Record bit 3	•
X1.5	•		Record bit 4	•
X1.6	•		Start	•
X1.7	•		Pause	•
X1.8	•		Mode	
X1.9	•		Brake Control	
X1.10	•		Enable	•
X1.11	•		Reset	•
X1.12		•	Motion Complete	•
X1.13		•	Start Acknowledgement	•
X1.14		•	Paused/Stopped	•
X1.15		•	Moving	
X1.16		•	Error	•
X1.17		•	parameterisable	
X1.18		•	parameterisable	
X1.19		•	In Zone	
X1.20		•	Referenced	•
X1.21		•	Ready	•
X1.22		•	Torque Limit Reached	

Table 6.1: CMMO-ST X1 interface inputs and outputs

The following routine puts the motor controller in the Ready status, which is mandatory for the following operations. The routine returns a TRUE value if the wanted status is reached. The first part of the code is populated by the necessary constants; the `timer_index` is used to specify which timer to use between the ones available for the robot, such timer is used to measure elapsed time to implement a timeout. The other constants are time intervals expressed in milliseconds that are needed as delay time or timeout. The routine begins with a `REPEAT UNTIL` loop, which repeats the instructions specified in it until a condition is verified; in this case, the condition that stops the loop, that has to be verified, is the high state of the `error_din` signal, which indicates that the motor controller has no errors. Inside the loop the timer is reset, then a `WAIT FOR` statement is used; it waits

for the high state of `error_din`, or for the timer to reach the specified timeout, either of the conditions makes the `WAIT FOR` instruction stop and proceed with the execution. With an `IF` statement it is checked if the waiting ended because the timeout is reached; in this case, an error message is generated with the `ERR_POST` function. Three parameters are provided to this function: the first integer indicates the number of the error, in this scope provisory values are used; the second is a string containing the error message that specifies that the motor controller is in an error state, the third parameter specifies the severity of the error. A value of two, which is the lowest available, is used; this produces a warning, but does not stop the execution of the routine, in this way it is possible to keep waiting for the wanted signal. At this point, the motor driver is expecting a high pause signal, which is provided by `$DOUT[pause_dout] := TRUE`, and should respond with a high paused signal. The same procedure is implemented to wait for this signal or for the expiration of the timer, using a `REPEAT UNTIL`, a `WAIT FOR`, and an `IF`. In this case the eventual error signals that the driver stays in the paused or stopped state. Now the controller enable signal is provided to the motor controller, a high ready signal is waited for as before; the error signals that the driver is not in the ready status. In the end of the routine a `TRUE` value is returned indicating that the ready status is reached.

```
1  ROUTINE establish_ready_status : BOOLEAN EXPORTED FROM
         GripperRoutines
2  ROUTINE establish_ready_status : BOOLEAN
3  CONST
4  timer_index = 1
5  t_2 = 1000
6  switch_on_timeout = 1100
7  paused_timeout = 1000
8  BEGIN
9  REPEAT
10 $TIMER[timer_index] := 0
11 WAIT FOR $DIN[error_din] = TRUE OR $TIMER[timer_index] >=
         switch_on_timeout
12 IF $TIMER[timer_index] > switch_on_timeout THEN
13     -- error the drive stays in error state
14     ERR_POST(43008, ' DRIVE STAYS IN ERROR STATE ',2)
15 ENDIF
16 UNTIL $DIN[error_din] = TRUE
17 $DOUT[pause_dout] := TRUE
18 REPEAT
19 $TIMER[timer_index] := 0
20 WAIT FOR $DIN[paused_din] = TRUE OR $TIMER[timer_index] >=
         paused_timeout
21 IF $TIMER[timer_index] > paused_timeout THEN
```

```
22      -- error the drive stays paused
23      ERR_POST(43008, ' DRIVE STAYS IN STOPPED STATE ',2)
24 ENDIF
25 UNTIL $DIN[paused_din] = TRUE
26 DELAY 100
27 $DOUT[ctrl_enable_dout] := TRUE
28 REPEAT
29 $TIMER[timer_index] := 0
30 WAIT FOR $DIN[ready_din] = TRUE OR $TIMER[timer_index] >= t_2
31 IF $TIMER[timer_index] >= t_2 THEN
32      ERR_POST(43008, ' DRIVE IS NOT READY ',2)
33 ENDIF
34 UNTIL $DIN[ready_din] = TRUE
35 RETURN (TRUE)
36 END establish_ready_status
```

The following routine can be used when the motor controller signals an error that can be acknowledged and thus ignored continuing the operations. After the `BEGIN` keyword, the Enable signal is switched off and the Reset signal is turned on. The motor controller should provide a high error signal indicating the absence of errors; the signal is waited for using the same `REPEAT UNTIL` instruction, in which the timer is reset and a `WAIT FOR` condition is used to check if the signal is received or the timer expires. In the latter case a warning is generated indicating that the error is not acknowledged. If the wanted signal is received, the execution continues, the controller enable signal is provided to the motor controller, and the ready signal response is waited for as before. In the end the routine returns a `TRUE` value indicating that the present error is acknowledged.

```
1  ROUTINE acknowledge_error : BOOLEAN EXPORTED FROM GripperRoutines
2  ROUTINE acknowledge_error : BOOLEAN
3  CONST
4  timer_index = 1
5  BEGIN
6  DELAY 100
7  $DOUT[reset_dout] := TRUE
8  $DOUT[ctrl_enable_dout] := FALSE
9  REPEAT
10      $TIMER[timer_index] := 0
11      WAIT FOR $DIN[error_din] = TRUE OR $TIMER[timer_index]>=2
12      IF ($TIMER[timer_index] > 2) THEN
13          -- error the error IS NOT aknowledged
14          ERR_POST(43008, ' ERROR IS NOT ACKNOWLEDGED',2)
15      ENDIF
16 UNTIL ($DIN[error_din] = TRUE)
17 $DOUT[ctrl_enable_dout] := TRUE
18 REPEAT
```

```
19      $TIMER[timer_index] := 0
20      WAIT FOR $DIN[ready_din] = TRUE OR $TIMER[timer_index] >= 10
21      IF ($TIMER[timer_index] >= 10) THEN
22          ERR_POST(43008, 'DRIVE IS NOT READY',2)
23      ENDIF
24  UNTIL ($DIN[ready_din] = TRUE)
25  $DOUT[reset_dout] := FALSE
26  RETURN (TRUE)
27  END acknowledge_error
```

The following routine performs the homing of the axis. The first `CONST` section is filled as before, a `VAR` section is added to declare all the needed variables, which in this case are an array of booleans, `record_selection_bn`, populated with the signal to be sent to the record selection bits, an array of integers, `record_bits_dout`, to store the mapped output points ports, and an integer `i` used in the for loop. After the `BEGIN` keyword the array of integer values are added, using the constant defined in the GripperRoutines program, then the `record_selection_bn` array elements are reset to zero or false state. This is done because the motor controller has to receive all zeros on the record selection bits to perform homing; subsequently the controller enable signal is provided to the motor controller and the ready signal is waited for as done in the other routines. With the next `FOR` loop the values contained in `record_selection_bn` are set on the corresponding output ports; a $2ms$ delay is needed for the motor controller after the record selection. After it, the start signal is sent from the robot; if this is received the motor controller responds with a start acknowledged signal. As before, the `REPEAT UNTIL` strategy is used to wait for this signal or post an error indicating that the start signal is not received. At this point it is checked that the motion complete signal is low, indicating that the motor is moving and, if so, the start signal is switched off. Then the routine waits for the motion complete and the referenced signals to be high with the same strategy; these signals indicate that the movement is completed and the axis is referenced. In the end the controller enable signal is switched off to activate the brake of the motor, and a `TRUE` value is returned indicating the correct homing.

```
1  ROUTINE do_homing : BOOLEAN EXPORTED FROM GripperRoutines
2  ROUTINE do_homing : BOOLEAN
3  CONST
4  timer_index = 1
5  homing_timeout = 20000 -- milliseconds
6  start_ack_timeout = 1000 -- milliseconds
7  t1_switch_on_delay = 1000 --milliseconds
8  VAR
9  record_bits_dout : ARRAY[5] OF INTEGER -- contains the mapped output
       points
```

94

```
10 record_selection_bn : ARRAY[5] OF BOOLEAN —— contains 5 bits for the
       index communication
11 i : INTEGER
12 BEGIN
13 record_bits_dout[1] := rec_bit_0_dout
14 record_bits_dout[2] := rec_bit_1_dout
15 record_bits_dout[3] := rec_bit_2_dout
16 record_bits_dout[4] := rec_bit_3_dout
17 record_bits_dout[5] := rec_bit_4_dout
18 FOR i:= 1 TO 5 DO
19     record_selection_bn[i] := FALSE      —— reset output bits array
20 ENDFOR
21 $DOUT[ctrl_enable_dout] := TRUE
22 REPEAT
23     $TIMER[timer_index] := 0
24     WAIT FOR $DIN[ready_din] = TRUE OR $TIMER[timer_index] >=
       t1_switch_on_delay
25     IF ($TIMER[timer_index] > t1_switch_on_delay) THEN
26         ERR_POST(43008, ' DRIVE IS NOT READY ',2)
27     ENDIF
28 UNTIL $DIN[ready_din] = TRUE
29 FOR i := 1 TO 5 DO
30     $DOUT[record_bits_dout[i]] := record_selection_bn[i]  —— toggle
       the corresponding binary value on the 5 $DOUTs
31 ENDFOR
32 DELAY 2   —— required delay
33 $DOUT[start_dout] := TRUE
34 REPEAT
35 $TIMER[timer_index] := 0
36 WAIT FOR $DIN[start_ack_din] = FALSE OR $TIMER[timer_index] >=
       start_ack_timeout
37 IF $TIMER[timer_index] > start_ack_timeout THEN
38     —— error the start command IS NOT acknowledged
39     ERR_POST(43008, ' START IS NOT ACKNOWLEDGED ',2)
40 ENDIF
41 UNTIL ($DIN[start_ack_din] = FALSE)
42 —— if the start is acknowledged the start command can be turned off
43 IF $DIN[motion_complete_din] = FALSE THEN —— it means that the axis
       is moving
44     $DOUT[start_dout] := FALSE
45 ENDIF
46 REPEAT
47 WAIT FOR $DIN[motion_complete_din] = TRUE AND $DIN[referenced_din] =
       TRUE OR $TIMER[timer_index] >= homing_timeout —— waits for the
       referenced or motion complete signals or for 20 seconds, if last
       case occours there is an error
48 IF ($TIMER[timer_index] > homing_timeout) THEN
49     ERR_POST(43008, ' HOMING TIMEOUT REACHED ',2)
50 ENDIF
```

```
51  UNTIL ($DIN[motion_complete_din] = TRUE AND $DIN[referenced_din] =
        TRUE)
52  $DOUT[ctrl_enable_dout] := FALSE
53  RETURN (TRUE)    -- the drive is referenced
54  END do_homing
```

The last routine moves the axis to the recording position specified by the parameter `targ_pos`; it returns `TRUE` if the movement is done correctly. The routine works in a similar way with respect to the homing one; the differences are in the position target definition and the expected signals from the motor controller. In the constant declarations section, the number of recorded positions stored on the motor controller is specified; in the variable declarations section, there are the same arrays used in the previous routine. An array containing all the recorded positions is added, the other variables are used in for loops, for the target position selection and for the binary conversion. After the `BEGIN` statement, the array of mapped output ports is populated as before, then the array of recorded positions is populated with the recorded positions; in this case, provisory values are used. The first phase consists of the comparison between the specified `targ_pos` and the positions already stored in the motor controller; this is done in a `FOR` loop over all the recorded positions, when the current evaluated value is smaller than `targ_pos`, assuming a movement of the slides from the inside to the outside of the box to have the suction cup inside the surface of the box, the value is stored along with the index that denotes it in the `recorded_positions` array. The variable `selected_index` indicates the record that has to be sent to the motor controller. After identifying the correct recording, its value is converted into a binary five bits value, populating the array `record_selection_bn`, the controller enable signal is sent to the motor controller to make sure that the brake is open. The ready signal is waited for as before, then all the digital output corresponding to the record selection input of the motor controller are set to zero; subsequently, it is checked that the controller is not paused with an `IF` condition, and in that case a warning is generated. To communicate the record selection, the values stored in `record_selection_bn` are set one by one in the `record_bits_dout` array using a `FOR` loop; after a $2ms$ delay the start signal is sent. As before, the routine waits for the start acknowledgment signal from the motor controller or for the expiration of the timeout; if the start command is acknowledged by the motor controller, the start signal is removed. The routine waits for the motion complete signal or for the timer to expire, returning `TRUE` if the movement is successful and activating the brake turning off the controller enable signal.

```
1  ROUTINE move_axis_to (targ_pos : REAL ) : BOOLEAN EXPORTED FROM
        GripperRoutines
2  ROUTINE move_axis_to (targ_pos : REAL ) : BOOLEAN
```

```
 3 CONST
 4 timer_index = 1
 5 start_ack_timeout = 10 —— milliseconds
 6 motion_timeout = 60000 —— milliseconds
 7 t1_switch_on_delay = 1000 ——milliseconds
 8 records_number = 5
 9 VAR
10 recorded_positions : ARRAY[records_number] OF INTEGER
11 record_bits_dout : ARRAY[5] OF INTEGER
12 record_selection_bn : ARRAY[5] OF INTEGER
13 closest_match : INTEGER
14 selected_index: INTEGER
15 dividend : INTEGER
16 quotient : INTEGER
17 i : INTEGER
18 BEGIN
19
20 record_bits_dout[1] := rec_bit_0_dout
21 record_bits_dout[2] := rec_bit_1_dout
22 record_bits_dout[3] := rec_bit_2_dout
23 record_bits_dout[4] := rec_bit_3_dout
24 record_bits_dout[5] := rec_bit_4_dout
25
26 recorded_positions[1] := 10 —— specify recorded positions
27 recorded_positions[2] := 20
28 recorded_positions[3] := 30
29 recorded_positions[4] := 40
30 recorded_positions[5] := 50
31
32 FOR i := 1 TO records_number DO
33     IF recorded_positions[i] <= targ_pos THEN
34         closest_match := recorded_positions[i]   —— if the value
      corresponds to the condition the value is overwritten
35         selected_index := i
36     ENDIF
37 ENDFOR
38 quotient := selected_index
39 FOR i:= 5 DOWNTO 1 DO
40     record_selection_bn[i] := quotient MOD 2
41     quotient := quotient DIV 2
42 ENDFOR
43 $DOUT[ctrl_enable_dout] := TRUE
44 REPEAT
45 WAIT FOR $DIN[ready_din] = TRUE OR $TIMER[timer_index] >=
      t1_switch_on_delay
46 IF ($TIMER[timer_index] > t1_switch_on_delay) THEN
47     ERR_POST(43008, ' DRIVER IS NOT READY ',2)
48 ENDIF
49 UNTIL ($DIN[ready_din] = TRUE)
```

```
50 FOR i := 1 TO 5 DO    —— set all the $dout for record selection to
        FALSE
51     $DOUT[record_bits_dout[i]] := FALSE
52 ENDFOR
53 IF ($DIN[paused_din] = FALSE) THEN
54     ERR_POST(43008, ' DRIVER IS STOPPED ',2)
55 ENDIF
56 FOR i := 1 TO 5 DO
57     IF record_selection_bn[i] = 1 THEN
58         $DOUT[record_bits_dout[i]] := TRUE —— toggle corresponding
        output
59     ELSE
60         $DOUT[record_bits_dout[i]] := FALSE
61     ENDIF
62 ENDFOR
63 DELAY 2
64 REPEAT
65 $TIMER[timer_index] := 0
66     WAIT FOR $DIN[start_ack_din] = FALSE OR $TIMER[timer_index] >=
        start_ack_timeout
67     IF ($TIMER[timer_index] > start_ack_timeout) THEN
68         —— the start IS NOT acknowledged
69         ERR_POST(43008, ' START IS NOT ACKNOWLEDGED ',2)
70     ENDIF
71 UNTIL ($DIN[start_ack_din] = FALSE)
72 DELAY 10
73 $DOUT[start_dout] := FALSE
74 REPEAT
75     $TIMER[timer_index] := 0
76     WAIT FOR $DIN[motion_complete_din] = TRUE OR $TIMER[timer_index]
        >= motion_timeout
77     IF ($TIMER[timer_index] > motion_timeout) THEN
78         ——error the movement took too long
79         ERR_POST(43008, ' MOTION NOT COMPLETED ',2)
80     ENDIF
81 UNTIL ($DIN[motion_complete_din] = TRUE)
82 $DOUT[ctrl_enable_dout] := FALSE
83 RETURN (TRUE) —— the movement IS completed
84 END move_axis_to
```

Chapter 7

Conclusions

The thesis proposes a solution for a flexible gripper composed of commercially available products and custom-designed parts. The aim of having a flexible product is obtained thanks to the exploitation of an electric actuator and defining different vacuum zones; custom-designed parts are tested via finite elements analyses, and a control strategy is implemented using PDL2 routines. The development of a real prototype in the future could check the correctness of the followed process and test the performances of the gripper. The robot-gripper connection, which is obtained through digital inputs and outputs discrete signals, can be developed into a less cabling-demanding solution; this would require the adoption of different components that use standardized communication protocols. Another solution that can be investigated is the adoption of a processing unit on the gripper itself; such a device could manage the suction cup positioning, vacuum generation, and monitoring.

Bibliography

[1] R. Mykhailyshyn, V. Savkiv, P. Maruschak, and J. Xiao. «A systematic review on pneumatic gripping devices for industrial robots». In: *Transport* 37.3 (Aug. 2022), pp. 201–231. DOI: https://doi.org/10.3846/transport.2022.17110 (cit. on pp. 2–7, 22, 24).

[2] Zakary Littlefield, Zhu Shaojun, Hristiyan Kourtev, Zacharias Psarakis, Rahul Shome, Andrew Kimmel, Andrew Dobson, Alberto F. De Souza, and Kostas E. Bekris. *Evaluating end-effector modalities for warehouse picking: A vacuum gripper vs a 3-finger underactuated hand.* 2016, pp. 1190–1195. DOI: 10.1109/COASE.2016.7743540 (cit. on pp. 7, 8).

[3] Junya Tanaka, Akihito Ogawa, Hideichi Nakamoto, Takafumi Sonoura, and Haruna Eto. «Suction pad unit using a bellows pneumatic actuator as a support mechanism for an end effector of depalletizing robots». In: *ROBOMECH Journal* 7 (2020). DOI: 10.1186/s40648-019-0151-0 (cit. on pp. 8–10).

[4] Aman Dhadge and Girish Tilekar. *Design of Enlarging Vacuum Gripper Using Slider Crank Mechanism.* 2020, pp. 52–57. DOI: 10.1109/ICCMA51325.2020.9301556 (cit. on pp. 10, 11, 22).

[5] Michael A Saliba, Andrew Vella Zarb, and Jonathan C Borg. «A modular, reconfigurable end effector for the plastics industry». eng. In: *Assembly automation* 30.2 (2010), pp. 147–154. ISSN: 0144-5154. DOI: 10.1108/01445151011029781 (cit. on pp. 11, 12, 22).

[6] Junya Tanaka and Akihito Ogawa. «Cardboard Box Depalletizing Robot Using Two-Surface Suction and Elastic Joint Mechanisms: Mechanism Proposal and Verification». In: *Journal of Robotics and Mechatronics* 31.3 (2019), pp. 474–492. DOI: 10.20965/jrm.2019.p0474 (cit. on pp. 13, 14).

[7] Anthony J. Bianculli. «Stepper motors: application and selection». In: *IEEE Spectrum* 7.12 (1970), pp. 25–29. DOI: 10.1109/MSPEC.1970.5213082 (cit. on p. 76).